We are IntechOpen, the world's leading publisher of Open Access books Built by scientists, for scientists

4,800
Open access books available

122,000
International authors and editors

135M
Downloads

Our authors are among the

154
Countries delivered to

TOP 1%
most cited scientists

12.2%
Contributors from top 500 universities

CLARIVATE ANALYTICS BOOK CITATION INDEX INDEXED

WEB OF SCIENCE™

Selection of our books indexed in the Book Citation Index in Web of Science™ Core Collection (BKCI)

Interested in publishing with us?
Contact book.department@intechopen.com

Numbers displayed above are based on latest data collected.
For more information visit www.intechopen.com

17

Photons as Working Body of Solar Engines

V.I. Laptev[1] and H. Khlyap[2]
[1]*Russian New University,*
[2]*Kaiserslautern University,*
[1]*Russian Federation*
[2]*Germany*

1. Introduction

Models of solar cells are constructed using the concepts of band theory and thermodynamic principles. The former have been most extensively used in calculations of the efficiency of solar cells (Luque & Marti, 2003; Badesku et al., 2001; De Vos et al., 1993, 1985; Landsberg & Tonge, 1989, 1980; Leff, 1987). Thermodynamic description is performed by two methods. In one of these, balance equations for energy and entropy fluxes are used, whereas the second (the method of cycles) comes to solutions of balance equations (Landsberg & Leff, 1989; Novikov, 1958; Rubin, 1979; De Vos, 1992).Conditions are sought under which energy exchange between radiation and substance produces as much work as possible. Work is maximum when the process is quasi-static. No equilibrium between substance and radiation is, however, attained in solar cells. We therefore believe that the search for continuous sequences of equilibrium states in solar energy conversion, which is not quasi-static on the whole, and an analysis of these states as separate processes aimed at improving the efficiency of solar cells is a problem of current interest. Examples of such use of the maximum work principle have not been found in the literature on radiant energy conversion (Luque & Marti, 2003; Badesku et al., 2001; De Vos et al., 1993, 1992, 1985; Landsberg & Tonge, 1989, 1980; Leff, 1987; Novikov, 1958; Rubin, 1979).

2. Theory of radiant energy conversion into work

2.1 Using model for converting radiant energy into work

We use the model of solar energy conversion (De Vos, 1985) shown in Fig. 1. The absorber of thermal radiation is blackbody *1* with temperature T_A. The blackbody is situated in the center of spherical cavity *2* with mirror walls and lens *3* used to achieve the highest radiation concentration on the black surface by optical methods. Heat absorber *4* with temperature $T_0<T_A$ is in contact with the blackbody.

The filling of cavity *2* with solar radiation is controlled by moving mirror *5*. If the mirror is in the position shown in Fig. 1, the cavity contains two radiations with temperatures T_A and T_S. If the mirror prevents access by solar radiation, the cavity contains radiation from blackbody *1* only. Radiations in excess of these two are not considered. In this model, solar energy conversion occurs at T_0= 300 and T_S = 5800 K. The temperature of the blackbody is T_A = 320 K.

2.2 Energy exchange between radiation and matter

2.2.1 Energy conversion without work production

It is known that the solar radiation in cavity *2* with volume V has energy $U_S=\sigma V T_S^4$ and entropy $S_s=4\sigma V T_S^3/3$, where σ is the Stefan-Boltzmann constant (Bazarov, 1964). The black body absorbs the radiation and emits radiation with energy $U_A=\sigma V T_A^4$ in cavity *2*. If T_A=320 K, these energies stand in a ratio of $U_S/U_A=(T_S/T_A)^4 \approx 10^6$, while $S_S/S_A=(T_S/T_A)^3 \approx 6\text{x}10^3$. As the volumes of radiations are equal, the amount of evolved heat ΔQ is proportional to the difference T_A^4-T_S^4 and is equal to the area under the isochore st on the entropy diagram drawn on the plane formed by the temperature (T) and entropy (S) axes in Fig. 2. The solar energy U_S entering the cavity and heat ΔQ are in ratio:

$$\eta_U = \Delta Q / U_S = (U_S - U_A)/U_S = 1-(T_A/T_S)^4. \quad (1)$$

Our model considers the value η_U as an efficiency of the photon reemission for a black body if the radiation and matter do not perform work in this process.

One should note that the efficiency of the photon absorption can be defined as (Wuerfel, 2005)

$$\eta_{abs} = 1-(\Omega_{emit}/\Omega_{abs})(T_A/T_S)^4,$$

where Ω is a solid angle for the incident or emitted radiation. In our case, the ratio $\Omega_{emit}/\Omega_{abs}$ can be ignored because value of η_U is close to one, for $(T_A/T_S)^4=(320/5800)^4 \approx 10^{-5}$. Thereafter we have to assume that $\eta_U = \eta_{abs.}$ The consequence is that solar energy can be almost completely transmitted to the absorber as heat if no work is done. Then a part of evolved heat ΔQ can be tranformed into work.

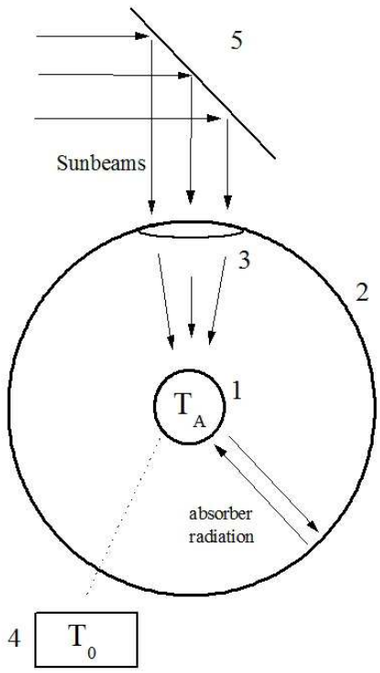

Fig. 1. Model of solar energy conversion from (Landsberg, 1978). Designations: 1. black body, *2*. spherical cavity, *3*. lens, *4*. heat receiver, *5*. movable mirror added by the author.

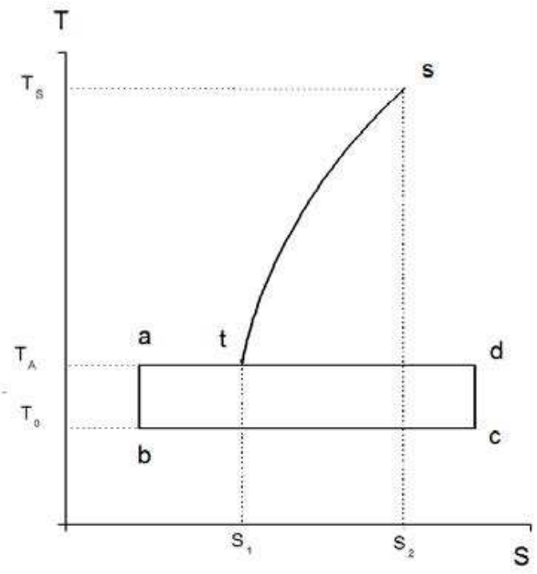

Fig. 2. Entropy diagram showing isochoric cooling of radiation (line st) in the cavity 2. The amount of evolved radiant heat is proportional to the area sts_ts_s. The amount of radiant heat converted into work is proportional to the area abcd. The work is performed by matter in a heat engine during Carnot cycle abcd.

2.2.2 Work production during the Carnot cycles

The absorbed radiant heat is converted into work by Carnot cycles involving matter as a working body. One such cycle is the rectangle abcd in Fig. 2. Work is performed during this cycle with an efficiency of

$$\eta_0 = 1 - T_0/T_A = 0.0625 \quad (2)$$

between the limit temperatures T_0=300 K and T_A=320 K.

It is common to say that the matter is the working body in this cycle. But radiation can be involved in the isothermic process ad in Fig. 2, because the efficiency of a Carnot cycle does not depend on kind and state of the working body. We will not discuss the properties of a matter-radiant working body. Let us simply note that a matter-radiant working body is possible. In this case upper limit of temperature T_A can reach 5800 K. The curve AB on Fig. 3 is the efficiency of this Carnot cycle where the matter cools down and heats up between temperatures T_A, T_0 and radiation has temperature T_A. In this cyclic process the matter and radiation are in equilibrium.

Let us show the absorption of radiation on an entropy diagram (Fig. 4) as an isothermal transfer of radiation from the volume V_2 of the cavity (state s) to the volume V_1 of the black body (state p). One can even reduce the radiation to state p* in Fig. 4. We will not discuss the properties of points p and p* here. Let us simply note that radiation reaches heat equilibrium with the black body (state e) from these points either through the adiabatic process p*e or through the isochoric process pe.

Let us represent the emission of radiation as its transfer from the volume of the black body (state e) to the volume V_2 of the cavity along the isotherm T_A (state t). As the radiation fills the cavity, it performs a work equal to the difference between the evolved and absorbed

heat. The radiation performs a considerable work if it reaches state t* on Fig. 3. Our calculations show that work is performed along the path sp*et* with an efficiency of

$$\eta_C = 1 - T_A/T_S = 0.945 \quad (3)$$

when T_A=320 K. It is important to note that, when radiation returns to its initial state s along the adiabat t*s, it constitutes a Carnot cycle with the same efficiency η_C.

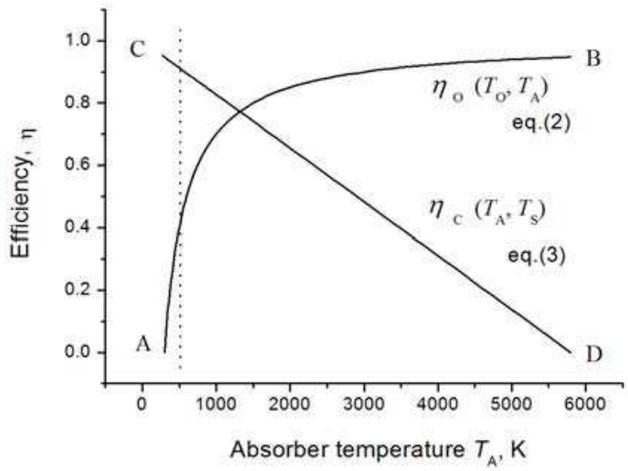

Fig. 3. Efficiencies of Carnot cycles in which the radiation takes place. The efficiency η_0 of work of radiation and matter in a cycle with temperatures limited at T_0 and T_A is shown as curve AB. Line CD shows the efficiency of a cyclic process where work is performed by radiation only.

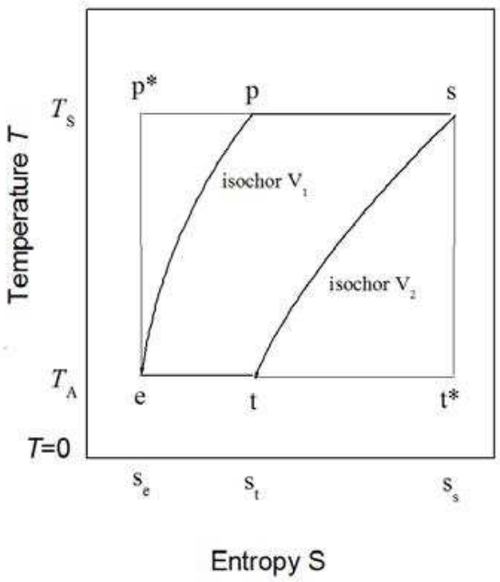

Fig. 4. Entropy diagram showing some thermodynamic cycles for conversion of solar heat into work in cavity *2* with the participation of a black body. Isotherms represent the absorption and emission of radiant energy. Lines pe, p*e correspond to the cooling of radiation in the black body. Line st indicates the temperature and entropy of radiation in cavity.

Fig. 3 compares work efficiencies η_0 and η_C during Carnot cycles described above. Radiation performs work during the Carnot cycle with a greater efficiency than η_0. η_0 and η_C values are calculated from Eqs. (2),(3) as a function of temperature T_A. We see that the efficiency η_C of conversion of heat into work in process with radiation only decreases with increasing temperature of the absorber, but the work efficiency η_0 of matter and radiation increases. Efficiencies are equal to 0.77 at T_A = 1330K.
Fig. 3 is divided in two parts by an isotherm at 500 K. On the left side is the region with temperatures where solar cells are used. The efficiency there of conversion of heat into work can reach value of 0.39 for a Carnot cycle with matter and be above 0.91 during a Carnot cycle with radiation. It is important to note, that other reversible and irrevesible cycles between these limit temperatures have efficiency smaller than efficiencies η_C or η_0.
The efficiency of parallel work done by radiation in the Carnot cycle sp*et*s (Fig. 4) and the matter in the Carnot cycle abcda (Fig. 3) is $\eta_0\eta_C$. It follows from (2) and (3) that

$$\eta_0\,\eta_C = (1-T_0/T_A)(1-T_A/T_S) = 0.0591.$$

After mathematical operations, it takes the form

$$\eta_0\,\eta_C = \eta_0+\eta_C -(1-T_0/T_S)= \eta_0+\eta_C-\eta_{OS},$$

where

$$\eta_{OS} = (1-T_0/T_S) \tag{4}$$

is the efficiency of the Carnot cycle in which the isotherm T_S corresponds to radiation and isotherm T_0, to the matter. Efficiency η_{OS} is independed from an absorber temperature T_A which divides adiabates in two parts. Upper parts of adiabates correspond to the change of radiation temperature, bottom parts to that of matter. It is important that such a Carnot cycle allows us to treat radiant heat absorption and emission as an isothermal and adiabatic processes performed by the matter. Efficiency η_{OS} is limiting for solar-heat engine. It is equal to 0.948 for limit temperatures T_0=300 K and T_S=5800 K. This Carnot cycle is not described in literature.

2.2.3 Work production during unlike Carnot cycles

Solar energy is converted as a result of a combination of different processes. Their mechanisms are mostly unknown. For this reason, one tries to establish the temperature dependence of the limit efficiency of a reversible combined process with the help of balance equations for energy and entropy flows. For solar engine, it takes the form (Landsberg, 1980; 1978)

$$\eta_{AS} = 1 - 4T_A/3T_S + T_A^4/3T_S^4. \tag{5}$$

For example, η_{AS} = 0.926 when T_A=320 K. Fig. 5 compares work efficiencies η_{AS} and η_C during the cycles with radiant working body at the same limit temperatures. η_{AS} and η_C values are calculated from Eqs. (3),(5) as a function of absorber temperature T_A. We see that $\eta_{AS} < \eta_C$, that is not presenting controversy to the Carnot theorem. The efficiencies η_{AS} and η_C of conversion of radiant heat into work decreases with increasing absorber temperature. The maximum difference η_C-η_{AS} is approx. 18% when T_A=3500 K (Landsberg, 1980; 1978).
The maximal value of the efficiency if for a black body at a temperature $T_A < T_S$ were possible to absorb the radiation from the sun without creating entropy is shown in (Wuerfel,

2005). It follows from a balance of absorbed and emitted energy and entropy flows under the condition of reversibility. The efficiency of a reversible process in which radiation and matter perform work is equal to

$$\eta_L = 1-(T_A/T_S)^4 - 4T_0\,[1 - (T_A/T_S)^3]/3T_S. \quad (6)$$

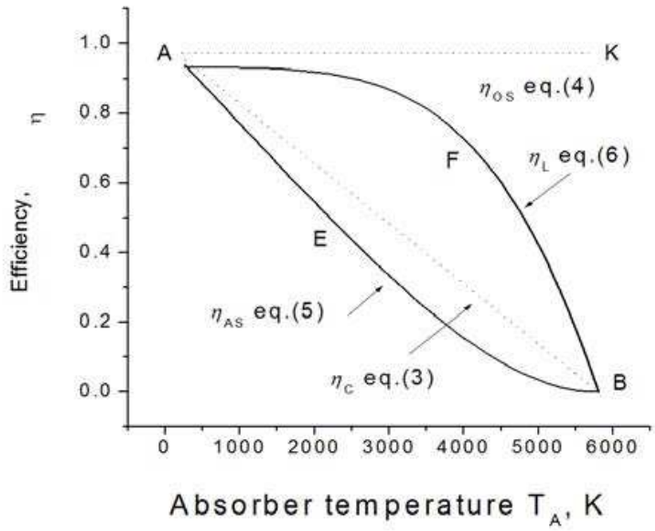

Fig. 5. Consideration of Carnot efficiencies and efficiencies of reversible processes other than the Carnot cycle. Dot lines AB,AK denote Carnot efficiencies η_C and η_{OS} at lower limit temperatures 320 and 300 K respectively. Solid curves AFB and AEB are efficiencies η_L and η_{AS} of non-Carnot engines at the same limit temperatures. Line AK and curve AFB discribe cycles with a radiant-matter working bodies. In the same time line AB and curve AEB describe cycles with radiant working body only.

For example, η_L = 0.931 when T_A=320 K and T_0=300 K. Condition T_0=T_A excludes temperature T_0 from expression (6) which in this case is described by the Eq. (5). It means that the work can be obtained during a cycle with a radiant and matter working bodies. Dependencies (5), (6) are shown in the Fig. 5 by curves AFB and AEB, respectively. Line AB presenting η_C from Eq. (3) and line AK presenting η_{OS} from Eq. (4) are also shown.

3. Elementary and matter-radiant working bodies

Two types of working body are considered:

- Elementary working body – matter or radiation in one cycle;
- Matter-radiant working body – matter and radiation in one cycle.

3.1 Energy conversion without irrevocable losses

According to Carnot theorem, an efficiency of a Carnot engine does not depend on a chemical nature, physical and aggregate states of a working body. The work presents a peculiarity of applying this theorem for solar cells. The statement is that the maximal efficiency of solar cells can be achieved with help of a combined working body only. Let's consider it in detail.

For example, the maximal efficiencies of the solar energy conversion are equal 94.8% at the limit temperatures 300 K and 5800 K (η_{OS} in the Table 1). Under these temperatures the efficiencies of the solar energy conversion can be equal 5.91% ($\eta_O\eta_C$ in Table 1). The one belongs to a Carnot cycle, in which a matter and radiation are found as a combined working body, i.e. matter and radiation as a whole system. The other belongs to 2 cycles running parallel. A matter performs the work with a low efficiency 6.25% (η_O in Table 1), but the radiation performs the work with a high efficiency 94.5% (η_C in Table 1). In these cases matter and radiation are elementary working bodies. The efficiencies of these parallel processes is

$$\eta_0\eta_C = 0.948 * 0.0625 = 0.0591 = 5.91\%.$$

Table 1 shows that a matter performs the work with a low efficiency in solar cells. However, the efficiency of the radiant work at the same absorber temperature is considerably higher. For example, a radiation performs the work with efficiency 92.6% during a non-Carnot cycle (η_{AS} in Table 1), but a matter produces work only with an efficiency 6.25% (η_0 in Table 1) at the absorber temperature 320 K. This difference is caused by various limit temperatures of the cycles (Table 1). The efficiencies of these processes running parallelis smaller than that of $\eta_0\eta_C$:

$$\eta_0\eta_{AS} = 0.926 * 0.0625 = 0.0579 = 5.79\%.$$

However, at the same temperatures the efficiency of solar energy conversion achieves 94.8% (η_{OS} in Table 1), if a work is performed during a cycle with the matter-radiant working body.

Classification of engines	**Efficiency at T_A = 320 K and other parameters of cycles**					
	Cycle	**Working body**	**Limit temperatures,K**	**Symbols**	**Limit, %**	**Calcilated equation**
Carnot engines						
heat	Carnot	Elementary / *matter or radiation*	300-320	η_0	6.25	2
solar	Carnot	elementary	320-5800	η_C	94.5	3
ideal solar-heat	Carnot	matter-radiation / *matter and radiation in one cycle*	300-5800	η_{OS}	94.8	4
non-Carnot engines						
solar	non-Carnot	elementary	320-5800	η_{AS}	92.6	5
solar- heat	non-Carnot	matter-radiation	300-5800	η_L	93.1	6
combined engines						
combined	Carnot, Carnot	elementary	300-320 320-5800	$\eta_0\eta_c$	5.91	2,3
combined	Carnot Carnot	elementary	300-320 300-5800	$\eta_0\eta_{OS}$	5.93	2,4
combined	Carnot, non-Carnot	elementary	300-320 320-5800	$\eta_0\eta_{AS}$	5.79	2,5
combined	Carnot, non-Carnot	elementary	300-320 300-5800	$\eta_0\eta_L$	5.82	2,6

Table 1. Classification and efficiencies of the engines with the elementary and matter-radiant working bodies

A Carnot cycle with the efficiency η_{OS} and the matter-radiant working body has been considered by the author earlier in the chapter, its efficiency is given by eq.4. Further we will call an engine with the matter-radiant working body an ideal solar-heat one. The elementary working bodies perform the work by solar or heat engines. Their properties are listed in Table 1. The advantage of the cyclic processes in comparison with the matter-radiant working body is obvious.

So, the elementary working bodies perform the work with the efficiencies η_0, η_C, η_L and η_{AS}. The matter-radiant working bodies perform the work with the efficiency η_{OS}. According to the Table. 1, one can confirm:

- a Carnot cycle with the matter-radiant working body has a maximally possible efficiency of solar energy conversion. It is equal 94.8% and does not depend on absorber temperature T_A. Engine where work is done during such cycle we will call an ideal solar-heat engine.
- electrical energy can be obtained under operating an ideal heat-solar engine with a very high efficiency and without additional function of low efficiency heat engine.

Therefore, high efficiency solar cells should be designed as solar-heat engine only.

3.2 Energy conversion with irrevocable losses

The absorption of radiation precedes the conversion of solar heat into work. In our model, the black body absorbs solar radiation and generates another radiation with a smaller temperature. Heat is evolved in this process; it is either converted into work or irrevocable lost. In this work the photon absorption in solar cells is divided into processes with and without work production. For the sake of simplicity, let us assume that heat evolved during solar energy reemission is lost with an efficiency of η_U from Eq. (1). The work of the cyclic processes is performed with the efficiencies of η_0, η_C, η_{AS}, η_{OS} and η_L (Tabl. 1). Then the conversion of solar heat with and without work production is performed with the efficiencies, for example, $\eta_C\eta_U$ or $\eta_0\eta_C\eta_U$. These and other combinations of efficiencies are compared in (Laptev, 2008).

It is important to note that the irrevocable energy losses of absorber at temperature 320 K do not cause the researchers' interest in thermodynamic analysis of conversion of solar heat into work. Actually, efficiency of the solar energy reemission as the irrevocable energy losses μ_U is close to 1 for $(T_A/T_S)^4 = (320/5800)^4 \approx 10^{-5}$. So efficiency of the solar energy reemission at 320 K has a small effect on efficiency of solar cell. The Tables 1,2 list efficiencies of the solar cells with and without irrevocable losses calculated in this work. The difference between these values does not exceed 0.01%. Values of $\mu_0\mu_C$ and $\mu_0\mu_C\mu_U$ may serve as examples. It might be seen that irrevocable energy losses are not to be taken into account in the thermodynamic analysis of conversion of solar heat into work. However, the detailed analysis of efficiencies of conversion of solar heat into work enabled us to reveal a correlation between the reversibility of solar energy reemission and efficiency of solar cell. The following parts of the chapter are devoted to this important aspect of conversion of solar heat into work.

3.3 Combinations of reversible and irreversible energy conversion processes

The temperature dependencies of μ_L from Eq. (5) and $\mu_0\mu_U$ from Eqs. (1),(2) are shown by lines LB, CB in Fig. 6. Let us also make use of the fact that every point of the line LB is (by definition) a graphical illustration of the sequence of reversible transitions from one energy state of the system to another, because each reversible process consists of the sequence of reversible transitions only.

Cycle parameters			Efficiency at T_A=320 K			
working body	**cycle**	**Limit temperatures,K**	**Symbols**	**Limit, %**	**eq-tion**	
non-working conversion						
-	reemission	320-5800	η_U	99.99	1	
heat, solar and heat-solar endoreversible engines						
elementary*	Carnot	300-320	$\mu_0\mu_U$	6.25	1, 2	
elementary	Carnot	320-5800	$\mu_C\mu_U$	94.5	1, 3	
elementary	non-Carnot	320-5800	$\mu_{AS}\mu_U$	92.6	1, 5	
matter-radiation**	non-Carnot	300-5800	$\mu_L\mu_U$	93.1	6	
matter-radiation	Carnot	300-5800	$\mu_{OS}\mu_U$	94.8	1, 4	
Combined endoreversible engines						
elementary	Carnot	300-320/320-5800	$\mu_0\mu_C\mu_U$	5.91	1, 2, 3	
elementary	Carnot/non-Carnot	300-320/320-5800	$\mu_0\mu_{AS}\mu_U$	5.79	1, 2, 5	
elementary	Carnot	300-320/300-5800	$\mu_0\mu_{0S}\mu_U$	5.93	1, 2, 4	
elementary	Carnot	300-320/320-5800/300-5800	$\mu_0\mu_C\mu_{0S}\mu_U$	5.60	1, 2, 3, 4	
elementary and matter-radiation	Carnot/non-Carnot	300-320/300-5800/320-5800	$\mu_0\mu_{0S}\mu_{AS}\mu_U$	5.49	1, 2, 4, 5	

* elementary working body – matter or radiation;
** matter-radiant working body – matter and radiation in one cycle.

Table 2. Classification and efficiencies of the engines with solar energy conversion as a irrevocably losses

Based on this statement one can say that every point of the line CB is (by definition) a graphical illustration of the sequence of reversible and irreversible energy transitions. First represent a Carnot cycle abcd in the Fig.2, second represent a process of cooling of radiation running according to the line st. This engine performs the work with the efficiency $\mu_0\mu_U$. The combination of reversible and irreversible processes allows us to call this engine an endoreversible. Engines with the efficiencies μ_L and μ_0 are reversible.
Curves CB и LB in Fig.6 have some dicrepancy because of the entropy production without a work production in endoreversible engine. Indeed reversible energy conversion with the efficiency μ_L or μ_0 occurs without entropy production. The energy conversion with efficiency μ_0 μ_U is accompanied by the entropy production during the solar energy reemissions. The latter ones do not take place in the work production and cause irrevocably losses.
So, the entropy is not performed during a reversible engines. Endoreversible engines perform the entropy. Thus, the author supposes that difference between efficiencies (μ_L- μ_0 μ_U) of these engines is proportional to the quality (or number) of irreversible transitions. In most cases the increase of number of irreversible transitions in conversion of radiant heat into irrevocably losses calls a reduce of the efficiency of engine from μ_L down to μ_0 μ_U.

Then, with help of the Fig. 6 one can find a ratio of reversible and irreversible transitions in a solar cell performing the work with the efficiency μ_0 μ_U. For example, let point *a* on Fig. 6 denote the conversion of solar energy with an efficiency of 30%. Let us draw an isotherm running through the point *a*; the intersections of this line with the line LB and the y-axis give us the values μ_L = 0.93 and T_A=430 K. Then, by the lever principle, the fraction of irreversible transitions q_{ir} in point *a* is

$$q_{ir} = (\mu_L\text{-}30)100/\ \mu_L = 68\%.$$

The fraction of irreversible transitions q_{rev} in point *a* will be 100–68=32%.
In other words, when in solar-heat engine (with the efficiency μ_L) 68% energy transitions can be made irreversible then the radiant work production will be ceased. If the reversible transitions (their number is now 32% of the total transitions' number) may form a Carnot cycle with the efficiency μ_0, then one can say that the reduce of number of reversible transitions leads to a cease of radiant work production, makes it possible to continue matter work production and reduces efficiency of engine from 93% down to 30%. The radiant heat evolved under these conditions partially takes a form of irrevocably losses as irreversible non-working transitions.

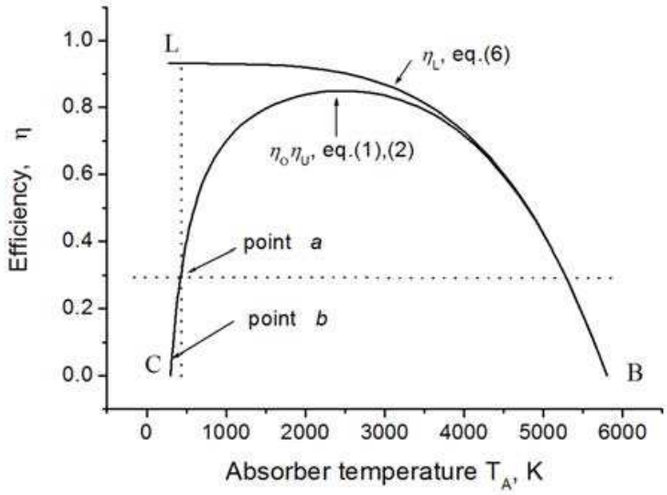

Fig. 6. Efficiency μ_L of solar-heat reversible engine (line LB) as a function of the absorber temperature T_A compared with the efficiency $\mu_0\mu_U$ of an heat endoreversible engine (line CB). Every point of the line LB correspond to 100% reversible transitions in energy conversion without entropy production. Every point of the line CB correspond to 100% irreversible transitions in energy conversion without work production. Every point of the region LBC between lines LB and CB correspond the reversible and irreversible transitions. Their parts can be found according to the lever's law (see text).

Let's consider a case of parallel work of matter and radiation. One could assume the work of radiation should increase an efficiency of solar-heat engine. However, it is not correct. The efficiencies of endoreversible processes whose elements are Carnot cycles with the efficiencies μ_C and μ_0 are shown in Fig. 7 by the CEB and CFB lines. They are situated below the LB line, whose every point is the efficiency μ_L of a reversible process by definition. We can therefore calculate the contributions of the Carnot cycle to the efficiencies μ_0 μ_U and μ_0

μ_C μ_U if the efficiency μ_L (μ-coordinates of line LB points) is taken as one. For example, the efficiency μ_0 μ_U at 320 K (point *b* in Fig.6) is 6.25% (Tabl.2). Let us draw an isotherm running through the point *b*; the intersections of this line with the line LB and the y-axis give us the value μ_L = 0.931. Then, by the lever principle, point *b* corresponds to a fraction

$$q_{ir} = (\mu_L\text{-}0.0625)100/\ \mu_L\text{=}93.3\%$$

of the irreversible transitions and the fraction q_{rev} = 6.7% of the reversible ones in conversion solar energy with the efficiency μ_0 μ_U=6.25%. If matter and radiation produce work with the efficiency μ_0 μ_C μ_U=5.91% at 320 K (Tabl.2), the fraction of irreversible transitions as irrevocably losses is

$$q_{ir} = (\mu_L\text{-}5.91)100/\ \mu_L\text{=}93.6\%.$$

The fraction of irreversible transitions q_{rev} of two Carnot cycles will be equal 100-93.6=6.4%. Thus, when matter and radiation produce work simultaneously in Carnot cycles, only less then 7% of energy transitions in solar energy conversion are working cycles. Remaining 97% of energy transitions in solar energy conversion are non-working processes. So, the efficiency of solar-heat engine sufficiently depends on the reversability of non-working processes, rather than on the efficiencies of the work cycles. Let's explain in more details.

3.4 Reversible and irreversible non-working processes

As it was mentioned above, the reason of descrepancy between curves μ_L, $\mu_0\mu_U$ and $\mu_0\mu_C\mu_U$ at T_A<T_S is entropy production during the processes without work production. Then the μ-coordinates of the points belonging to the plane between line μ_L and the lines $\mu_0\mu_U$, $\mu_0\mu_C\mu_U$ on Fig. 7 are proportional to the shares of the reversible and irreversible transitions without work production. We propose the following method for calculating relative contributions of reversible and irreversible processes without work production.

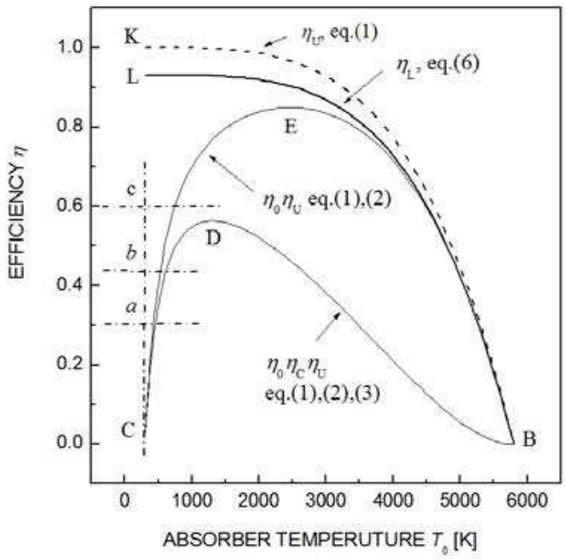

Fig. 7. The comparison of the well-known thermodynamic efficiency limitations of the solar energy conversion with and without entropy production.

The temperature dependencies of μ_L, $\mu_0\mu_U$, $\mu_0\mu_C\mu_U$ derived from Eqs. (1),(2),(3) and(6) are shown by lines LB, CEB and CDB in Fig. 7. Remember that the μ-coordinates of the points belonging to the lines $\mu_0\mu_U$, $\mu_0\mu_C\mu_U$ are proportional to the shares of reversible transitions which are one or two Carnot cycles with the efficiencies μ_0 and μ_C. At the same time remaining 100% irreversible transitions are (form) irreversible processes without work production as irrevocably losses.

The lines CEB and CDB on Fig. 7 are not only the illustration of possible ways of converting solar energy. For example, it is known that the limiting efficiencies of solar cells on the basis of a p,n-transition are 30% (Shockley & Queisser, 1961) and 43% (Werner et al., 1994). at T_A=320 K. They are shown by points *a* and *b* on Fig. 7 and lie above the lines $\mu_0\mu_U$, $\mu_0\mu_C\mu_U$, but below the line μ_L. One can say that processes without work production may be the combination of reversible and irreversible processes running parallel. Then the μ-coordinates of the points above the lines CEB, CDB are proportional to the shares q of reversible and irreversible transitions, which are appearing as processes without work production. According to the lever's principle, fraction of irreversible transitions q_{ir} in conversion of solar energy is

$$q_{ir} = (\mu_L - \mu_0\mu_C\mu_U)100/\mu_L.$$

For example, according to Tabl. 1,2, μ_L=93.1% and $\mu_0\mu_C\mu_U$=5.91% at T_A=320 K. Then q_{ir} = (93.1-5.91)100/93.1=93.7%. The fraction of reversible transitions q_{rev} is 100-93.7=6.3%.

Point *a* in Fig.7 denotes the conversion of solar energy with an efficiency μ=30% at T_A=320 K. It lies above the line $\mu_0\mu_C\mu_U$. Then the value

$$q_{ir} = (\mu_L - \mu)100/(\mu_L - \mu_0\mu_C\mu_U)$$

is a part of irreversible transitions in the conversion of solar energy without work production. In our case it is (93.1-30)100/(93.1-5.91)=70.0%. The fraction of reversible transitions will be equal to 100-70.0=30.0%. Note that there are no reversible transitions of Carnot cycles.

The band theory proposes mechanisms of converting solar energy into work with an efficiency of 43% (Landsberg & Leff, 1989). Let us denote last value by the point *b* on the isotherm in Fig. 7. Then the fraction of irreversible transitions q_{ir} without work production is (93.1-43)100/(93.1-5.91)= 57.5%, and the fraction of reversible transitions q_{rev} without work production will be equal 100-57.5=42.5%. So that, to increase efficiency of endorevesible solar-heat engine from 30 up to 43% at T_A=320 K, it's necessary to reduce a fraction of irreversible transitions without work production from 72.4% down to 57.5%.

As an example of reverse calculations let's find out efficiency of solar-heat engine with 50% irreversible transitions without work production. Denote the value is to be found as x and write down the equation

$$q_{ir} = (93.1 - x)100/(93.1 - 5.91) = 50\%.$$

Solving it reveal that x=49.5%. Note that for q_{ir} = 100% efficiency $\mu_0\mu_C\mu_U$=50% may be achieved only under T_A=700 K (see Fig.7). This temperature is much higher than the temperatures of solar cells' exploitation (the temperatures of solar cells' working conditions) Thus, the author supposes the key for further increase of solar cells' efficiency is in the study and perfecting processes without work production.

3.5 Ideal solar-heat engines

According to the Eqs. (4),(6), there are two efficiency limits of solar energy conversion in reversible processes for a pair of limiting temperatures T_0 and T_S, namely, μ_{OS}, μ_L. In the Fig. 8 are shown their dependencies on absorber temperature T_A. Obviously, under all values of T_A the condition $\mu_{OS} > \mu_L$ is fulfilled. The suggestion can be made that processes can occur whose efficiency is between these limits. By virtue of the second law of thermodynamics, they cannot be reversible.

For instance, radiant energy conversion with the efficiency $\mu_{OS}\mu_U$ is irreversible, because radiation performs an irreversible process with the efficiency μ_U along the line st shown in Fig. 2. We see from Fig. 8 that the μ_{OS} μ_U values (line AB) at temperatures $T_A << T_S$ are indeed larger than μ_L (line LB) and smaller than μ_{OS} (line AD).

In each point of the line AB the irreversible processes appeare as a sequence of transitions without work production. Because the efficiency μ_{OS} μ_U of the processes with their participation larger then μ_L, one can suppose that the fraction of irreversible transitions along the line LB is equal to zero, and along the line AB is equal to unity. In the plane between lines AB и LB the fraction of irreversible transitions q_{ir} may be calculated according to the lever principle:

$$q_{ir} = (\mu_{OS}\mu_U - \mu)100/(\mu_{OS}\mu_U - \mu_L).$$

In each point of the line AB the fraction of irreversible transitions q^0_i of total number of irrevesible transitions is

$$q^0_{ir} = (\mu_{OS}\mu_U - \mu_L)100/(\mu_S\mu_U).$$

According to the Tables 1, 2, q^0_{ir}=1.8% at T_A=320 K. The processes consisting of these transitions, do not produce work.

So, along the line AD (Fig. 8) conversion of solar energy is perfomed during a Carnot cycle, along the line AB – during a Carnot cycle and the processes without work production. In the plane between these lines only work is perfomed. The working process is a non-Carnot cycle.

Between the lines AB and LB non-working processes are reversible and irreversible. There the fraction of irrevesible transitions decreases with closing the line LB. Along the line LB all energy transitions (with and without work production) are reversible, i.e. q^0_{ir}=0.

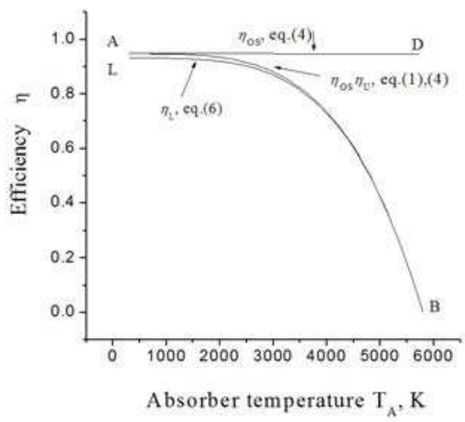

Fig. 8. Comparison of the efficiency $\mu_{OS}\mu_U$ of combinations of reversible working and irreversible non-working processes (the AB line) with the efficiency μ_{OS} of a reversible Carnot working process (the AD line) and the efficiency μ_L of reversible non-Carnot working processes (the LB line). Lines AD и AB coincide at T_A=0 K.

Irreversible processes without work production appear under the line LB. Their fraction increase as we move off the line LB. The previous chapter gives examples of calculating their contributions to solar energy conversion.

The value μ_L is a keyword in separation of solar energy conversion in processes with and without work production. It is referred as Landsberg efficiency (Wuerfel, 2005). According to this tradition, solar-heat engine with the efficiency μ_L are called Landsberg engine. It has a minimal efficiency of all solar-heat engines.

Solar-heat engine with the maximal efficiency μ_{OS} we call ideal solar-heat engine. Then solar-heat engine with the efficiency between μ_{OS} и $\mu_{OS}\mu_U$ may be noted as ideal non-Carnot solar-heat engine, and a solar-heat engine with the efficiency between $\mu_{OS}\mu_U$ and μ_L as an endoreversible solar-heat engine.

Solar-heat engine have cycles with the matter-radiant working body. We will not discuss the properties of the matter-radiant working body here. Let us simply note that all energy transitions in solar-heat engines are performed by the matter-radiant working body (Table 3). In the endoreversible solar-heat engine the matter-radiant working body makes working transitions, their fraction of total number of energy transitions is 100-1.8=98.2% because the processes without work production have only 1.8% energy transitions. Engine with the matter-radiant working body is not produced yet.

Engine	*Efficiency at 320 K*	*contributions of energy transitions, %*		*matter and radiation state*
		working	*non-working*	
Idel Carnot solar-heat	94.80	100	-	equilibrium
Ideal non-Carnot solar-heat	94.79	100	-	equilibrium
Endoreversible solar-heat	93.10-94.79	98.2	1.8	Non-equilibrium
Landsberg reversible	93.10	< 7	>93	equilibrium
Combined endoreversible	<6	< 7	>93	Non-equilibrium

Table 3. Comparison between the engine efficiencies and the contributions of working and non-working transitions

Existent solar cells are endoreversible combined engines with the non-Carnot cycles and elementary working bodies (matter or radiation). The working bodies perform working energy transitions, their fraction (as it is shown in the Table 3) can achieve only 7 % of transitions total number. We cannot overcome this 7% barrier but it doesn't mean that there is no possibility to increase the efficiency of such a machine. According to the Table 3, the non-working transitions are more than 93% from the total number of energy transitions. They can be either irreversible or revesible. If the first are made as the last, the engine efficiency can be increased from 6 up to 93.1%. So the aim of perfection in endoreversible solar-heat engine processes without work production is arisen. In ideal case it is necessary to obtain Landsberg engine.

So, efficiencies of the combined endoreversible engines with the non-Carnot cycles and elementary working bodies (matter or radiation) mostly depend on reversibility of processes without work production, running in the radiation absorber rather than on the work

production processes. It follows that the contribution of reversible processes is smaller than the contribution of irreversible processes in devices that are currently used. According to the maximum work principle, their efficiency can be increased by increasing the fraction of reversible processes in solar energy absorbers. The following approach to solution of this problem can be suggested.

4. Antenna states and processes

Antenna states of atomic particles or their groups are the states between them resulting from the reemission of photons without work production and heat dissipation. Below is shown that a comparison of the efficiencies of the reversible and irreversible photon reemissions occuring in parallel made it clear that it is impossible to attain very high efficiencies in the conversion of solar heat into work without the reversible photon reemissions as antenna process.

4.1 Photon reemissions as non-working processes

Matter and solar radiation are never in equilibrium in solar cells and quasi-static conversion of the solar energy is not achieved. For this reason, the irreversible thermodynamic engines are described using the method of endoreversible thermodynamics of solar energy conversion (Novikov, 1958; Rubin, 1979; De Vos, 1992). Remember that endoreversible engines are irreversible engines where all irreversibilities are restricted to the coupling of engine to the external world. It is assumed that the inner reversible part of an endoreversible engine is a Carnot cycle. We have also considered the non-Carnot cycles and found out that photon absorption in solar cells can be considered as the external reversible part of an endoreversible engine.

The photon absorption in solar cells is separated into processes with and without work production. These processes are sequencies of transitions from one energy state of the system to another. The energy transitions between particle states are called "photon reemission" if they do not take part in performing work and heat dissipation.

The photon reemission is divided into reversible and irreversible processes. These non-working processes are regarded as a continuous series of equilibrium states outside the irreversible or endoreversible engine, are isolate into separate processes, and are used to obtain a higher efficiency of the generally non-quasistatic solar energy conversion. We can consider those equilibrium processes as a base of the „exoreversible“additional device for the irreversible or endoreversible engine.

So, we have called the processes without work production photon reemission. Let us now shown that they play a special role in the conversion of solar heat into work.

4.2 Antenna states of the absorber particles

Let us consider these particle states in a radiant energy absorber, transitions between them result from the absorption of photons. The states of atomic particles or their groups, as well as energy transitions between them, are called "working" if they take part in performing work. It is known that solar energy conversions are not always working processes. The states of atomic particles and the energy transitions between them are said to be "antenna" ones if they take part in the absorption and emission of radiant energy without work production, i.e. in the photon reemission. Carnot cycles are examples of working processes, while cycles described below involving the photon reemission are examples of antenna processes.

It is clear that antenna and working states are equilibrium ones if cycles of the radiant energy conversion are not accompanied by entropy production, i.e. if it takes place along line LB on Fig. 9 with an efficiency μ_L from Eq. (5). Let us take their total amount to be 100%. Now assume that the conversion of radiant energy consists of reversible working processes with an efficiency μ_O from Eq. (2) for matter, with an efficiency μ_{AS} from Eq. (5) for radiation and irreversible with an efficiency μ_U from Eq. (1) for irreversible antenna processes, i.e. that the conversion of radiant energy corresponds to line CEB. In this case, the μ-coordinates of all points belonging to the line CEB divided by μ_L are equal to the fraction of working states, while $1-\mu/\mu_L$ is equal to the fraction of antenna non-equilibrium states.
Fig. 9 shows that the number of antenna non-equilibrium states in solar cells decreases as the efficiency μ grows along lines CE and CF. The isothermal growth of the efficiency μ implies that the total amount of antenna states remains constant, but certain antenna states have become equilibrium states and that reversible transitions that do not generate work have appeared. If the temperature dependence of μ is determined by experiment, Fig. 9 becomes in our opinion an effective tool for interpreting and modeling the paths along which work is performed by solar cells. We can consider Fig. 9 as the reversibility diagram of the conversion of solar heat into work.

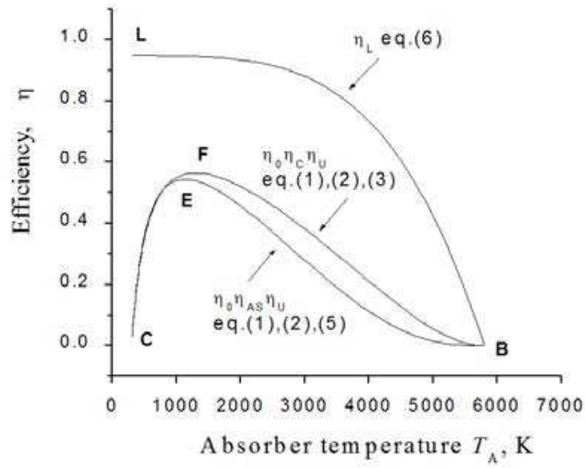

Fig. 9. Comparison of the efficiency μ_L of Landsberg engine (the LB line) with the efficiencies of combined engines (the CEB, CFB lines). A difference between the efficiencies $\eta_0\eta_{AS}\eta_U$ and $\mu_O\mu_C\mu_U$ is that in the first case radiation working cycle is not a Carnot cycle. Lines CEB and CFB are practically coincide at temperatures used for operation of solar cells.

Obviously, knowledge of physical and chemical nature of antenna states of particles is important for revealing optimal schemes for radiant energy conversion. The question about technical realization of antenna states is not subject of this chapter. This is a material science problem. One only should note the model of absorber with antenna states does not contradict to thermodynamic laws and represents a way of solution of following aim: how to separate any given cycle into infinite number of infinitely small arbitrary cycles.

4.3 Antenna processes

The absorption and generation of photons in the abcd (Fig. 2) and spet (Fig. 4) processes is accompanied by the production of work. No work is done in the st process (Fig. 2). This

difference can be used to divide all processes with the absorption and generation of photons into two types. The first type includes processes in which the matter and radiation do work, that is, participate in the working process. The second type includes processes in which the substance absorbs and emits radiant energy without doing work, that is, participates in an antenna process. The spontaneous evening out of the temperatures of the matter and radiation is an example of antenna processes, and radiant energy conversion in a solar cell is a combination of processes of the first and second type.

The highest efficiency of a combination of work and antenna processes is described by the line AB in Fig. 8. If the work is performed during a non-Carnot cycle then efficiency of the work and antenna processes is described by the LB line. The difference between $\eta_{OS}\eta_U$ and η_L is 94.8-93.1=1.7%. For analysis of antenna processes one should choose the temperature dependence of the value η_L because in this case a conversion process is reversible.

The CEB line in Fig.9 shows the efficiency of a combination of work done by matter (in a Carnot cycle with the efficiency η_0), by radiation (in a non-Carnot cycle with the efficiency η_{AS}) and a background antenna process with the efficiency η_U. The η coordinates of the CEB line divided by η_L describe the largest contribution of working processes to the efficiency of solar energy conversion if η_L is taken as one. The contribution of the antenna process is then $1- \eta_0\eta_{AS}\eta_U/\eta_L$.

It follows that the efficiency of conversion higher than $\eta_0\eta_{AS}\eta_U$ (the region between the LB and CEB lines, Fig. 9) can be obtained by perfecting the antenna process only. The efficiency of solar energy conversion is maximum in this case if all antenna processes are reversible. The efficiency is minimum if all antenna processes are irreversible.

The η coordinates of points between the LB and CEB lines are then proportional to the fraction of reversible antenna processes. An irreversible antenna process corresponds to the $1 - \eta/\eta_L$ value. The character of this dependence will not be discussed here. Only note that Fig. 9 can be used to calculate the fractions of work and antenna processes, as well as contributions of reversible and irreversible antenna processes in solar energy conversion if experimental data on the temperature dependence of the solar cell efficiency are available.

So, the antenna processes in Landsberg engine are reversible. When antenna processes are made irreversible, then the efficiency of transformation of radiant energy decreases from η_L=94.8% down to $\eta_0\eta_{AS}\eta_U$=5.79% at T_A=320 K. We have to select the opposite way.

4.4 Photon reemissions as reversible antenna processes

The notion of the reversibility of a process is applicable to any thermodynamic system, although we have not found it applied to quantum systems in physical literature. Let us recall that the transition of a system from equilibrium state 1 to equilibrium state 2 is called reversible (i.e., bi-directional) if one can return from state 2 to state 1 without making any changes in the surrounding environment, i.e. without compensations. The transition of a system from state 1 to state 2 is said to be irreversible if it is impossible to return from state 2 to state 1 without compensations.

Let us consider these particle states in an absorber, transitions between them result from the absorption of photons. The state of radiation will not change if the photon reemissions (121) or (12321) can take place (Fig. 10). These reemission processes will be reversible ones if the equilibrium state of matter is not violated by a photon absorption. According to these definitions, the reemission (123) or (1231) will alter the frequency distribution of photons (Fig. 11). For this reason, such reemission processes are irreversible.

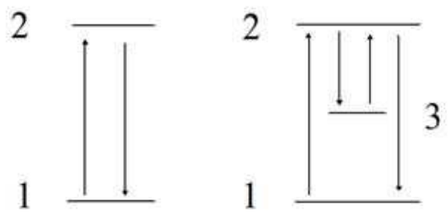

Fig. 10. The reversible reemissions in the systems with 2 and 3 energy levels.

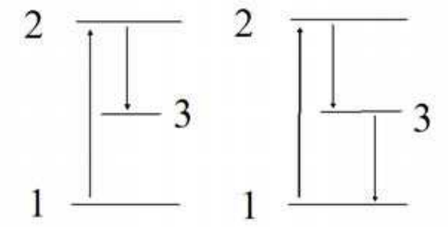

Fig. 11. The irreversible reemissions in the systems with 3 energy levels.

4.5 Photon reemissions as quasi-static process

Every quasi-static process is reversible and infinitely slow. Are the continuous series of the photon reemissions $(121)_n$ and $(12321)_n$ quasi-static processes? For the sake of simplicity, let us approximate the spatial arrangement of particles by a periodic chain of elements that have a length of 2μm (absorber thickness) and that are separated by 2 Å (atomic distance). Use the identity of electronic states 1, 2, 3 in particles **A** and present the sequence of electronic excitations in the particles' chain with help of reemission cycles in the Figs. 10, 11, for example, as follows:

$$\begin{aligned}
&\mathbf{A}_1+h\upsilon_{12}\rightarrow \\
&\quad\rightarrow\mathbf{A}_{1\rightarrow2\rightarrow1}+h\upsilon_{21}\rightarrow \\
&\qquad\rightarrow\mathbf{A}_{1\rightarrow2\rightarrow3\rightarrow1}+h\upsilon_{23}+h\upsilon_{31}\rightarrow \\
&\qquad\qquad\rightarrow\mathbf{A}_{1\rightarrow3\rightarrow1}+h\upsilon_{31}\rightarrow \\
&\qquad\qquad\qquad\rightarrow\mathbf{A}_{1\rightarrow3\rightarrow2\rightarrow1}+h\upsilon_{21}\rightarrow \ldots. \\
&\qquad\qquad\qquad\qquad\rightarrow \mathbf{A}_{1\rightarrow2\rightarrow1}+h\upsilon_{21}
\end{aligned} \tag{7}$$

In this expression the first particle is excited by the photon with energy $h\upsilon_{21}$ and emits the same photon. This emitted photon excites the second particle, which emits two photons with energies $h\upsilon_{23}$ and $h\upsilon_{31}$. They, in turn, excite the third particle and so on.

The time period during which solar radiation will excite only the first particle in the chain, while subsequent particles are excited only by reemitted photons, is equal to 10^{-4} s if the lifetime of the excited state is ~10^{-8} s. The time needed for the wave to travel down the chain and excite only the last particle is ~10^{-14} s. These time intervals are related to each other as 320 years to one second. Therefore, the energy exchange due to reemission in a chain of particles is an infinitely slow process in comparison with the diffusion of electromagnetic radiation in the chain. Even the multiple repetition of reemission (121) by one particle during ~10^{-6} s is an infinitely slow process, the time taken by such reemission exceeds the lifetime of the excited states by a factor of 100.

The radiant energy conversion may be characterized by the variable ratio of numbers of reversible and irreversible processes. In the chain (7) this ratio depends on (as shown in Figs. 10, 11) the order of states 1, 2, 3 alternation in cycle of each particle **A**. The index of **A** points it out. In general case we do not know either the reemission number, or states number in the cycle of reemission, as well as their alternation. But formally we can make a continuum consisting of all reversible cycles of the chain (7) and photons of reemission. Separate the reversible cycles and photons by brackets and right down the following expression:

$$(\mathbf{A}_{1\to2\to1} + h\upsilon_{21} + \mathbf{A}_{1\to3\to1} + h\upsilon_{31} + \mathbf{A}_{2\to3\to2} + h\upsilon_{32} + ...) +$$

$$\mathbf{A}_{1\to2\to3\to1} + h\upsilon_{23} + h\upsilon_{31} + \mathbf{A}_{1\to3\to2\to1} + h\upsilon_{32} + h\upsilon_{21} \quad (8)$$

The particles with irreversible reemission cycles are out of brackets.
The sequence of particles states in brackets may be thought as infinite one. (Note that if only one particle were in the brackets, then manifold repetition of its cycle might be considered as an infinite sequence of equilibrium states). In the solid absorber one can select a big number (~10^{19}) of chains consisting of these particles. While the quasistatic process is by definition an infinite and continous sequence of equlibrium states, then there is a fundamental possibility to consider local quasistatic processes in the whole irreversible process of radiant energy transformation.
Thus the sequences of photon reemissions of absorber particles in solar cells can take the form of quasi-static processes. Their isolation out from the general process of the conversion of solar energy into work (which is a non-equilibrium process on the whole) does not contradict the laws of thermodynamics.

4.6 Antenna processes and temperature of radiation

Let us call the reemission of solar energy during an antenna process *retranslation*, if the temperature of the radiation remains constant, and *transformation*, if the temperature of the radiation changes. The retranslation of radiation by a black body is, by definition, a reversible process. Transformation can take place both in a reversible and irreversible way. Therefore, the efficiency of the work performed by a solar cell can be improved by increasing the fraction of retranslating and transforming reversible antenna processes as well as working equilibrium states in an absorber.

4.7 Antenna processes and photon cutting

A photon cutting process (Wegh et al., 1999) as photon reemission is an example for an antenna process. It includes the emission of two visible photons for each vacuum ultraviolet photon absorbed. For us important, that materials with introduced luminescent activators ensure the separation of the photon antenna reemissions and the photon work production processes. In our opinion, ultra-high efficiencies can be reached if: firstly, we solve the problem of separating the photon antenna reemissions and the photon work production processes. Secondly, one should know a way of transformation of irreversible photon antenna reemissions into reversible. Let us consider the activator states in an absorber as state 3. A photon cutting process is irreversible in case of the reemissions $(1231)_n$. They can be luminescent. A photon cutting process can be reversible if an activator performs the reemissions $(1231321)_n$. They cannot be luminescent. An absorber with such activators can resemble a black body. Therefore, photon cutting processes can also play a role in transformation of irreversible reemission into reversible. This way is one of many others.

4.8 Antenna processes in plants

Let us leave the discussion of technological matters relating to the manipulation of antenna processes aside for the time being. We will devote a subsequent publication to this subject. Let us only remark here that the conversion of solar energy involving the participation of antenna molecules figures in the description of photosynthesis in biology. Every chlorophyll molecule in plant cells, which is a direct convertor of solar energy, is surrounded by a complex of 250-400 pigment molecules (Raven et al., 1999). The thermodynamic aspects of photosynthesis in plants were studied in (Wuerfel, 2005; Landsberg, 1977), yet the idea of antenna for solar cells was not proposed. We hope that the notions of the antenna and working states of an absorber particles will make it possible to attain very high efficiencies of the radiant energy convertors, especially in those cases when solar radiation is not powerful enough to make solar cells work efficiently yet suffices to drive photosynthesis in plants.

4.9 Conclusion

This leads us to conclude that reemission of radiant energy by absorbent particles can be considered a quasi-static process. We can therefore hope that the concept of an antenna process, which is photon absorption and generation, can be used to find methods for attaining the efficiency of solar energy conversion close to the limiting efficiency without invoking band theory concepts.

5. Thermodynamic scale of the efficiency of chemical action of solar radiation

Radiant energy conversion has a limit efficiency in natural processes. This efficiency is lower in solar, biological and chemical reactors. With the thermodynamic scale of efficiency of chemical action of solar radiation we will be able to compare the efficiency of natural processes and different reactors and estimate their commercial advantages. Such a scale is absent in the well_known thermodynamic descriptions of the solar energy conversion, its storage and transportation to other energy generators (Steinfeld & Palumbo, 2001). Here the thermodynamic scale of the efficiency of chemical action of solar radiation is based on the Carnot theorem.

Chemical changes are linked to chemical potentials. In this work it is shown for the first time that the chemical action of solar radiation **S** on the reactant **R**

$$\mathbf{R} + \mathbf{S} \leftrightarrow \mathbf{P} + \mathbf{M} \tag{9}$$

is so special that the difference of chemical potentials of substances R and P

$$\mu_R - \mu_P = f(T) \tag{10}$$

becomes a function of their temperature even in the idealized reverse process (9), if the chemical potential of solar radiation is accepted to be non-zero. Actually, there are no obstacles to use the function $f(T)$ in thermodynamic calculations of solar chemical reactions, because in (Kondepudi & Prigogin, 1998) it is shown that the non–zero chemical potential of heat radiation does not contradict with the fundamental equation of the thermodynamics. The solar radiation is a black body radiation.

Let us consider a volume with a black body R, transparent walls and a thermostat T as an idealized solar chemical reactor. The chemical action of solar radiation S on the reactant R will be defined by a boundary condition

$$\mu_R - \mu_P = \mu_m - \mu_S = f(T), \tag{11}$$

where μ_m is a chemical potential of heat radiation emitted by product P. Then the calculation of the function $f(T)$ is simply reduced to the definition of a difference $(\mu_m - \mu_S)$, because chemical potential of heat radiation does not depend on chemical composition of the radiator, and the numerical procedure for μ_m and μ_S is known and simple (Laptev, 2008).

The chemical potential as an intensive parameter of the fundamental equation of thermodynamics is defined by differentiation of characteristic functions on number of particles N (Laptev, 2010). The internal energy U as a characteristic function of the photon number

$$U(V,N) = (2.703Nk)^{4/3}/(\sigma V)^{1/3}$$

is calculated by the author in (Laptev, 2008, 2010) by a joint solution of two equations: the known characteristic function

$$U(S,V) = \sigma\, V(3S/4\, \sigma\, V)^{4/3}$$

(Bazarov, 1964) and the expression (Couture & Zitoun, 2000; Mazenko, 2000)

$$N = 0.370\, \sigma T^3 V/k = S/3.602\, k, \tag{12}$$

where T, S, V are temperature, entropy and volume of heat radiation, σ is the Stephan–Boltzmann constant, k is the Boltzmnn constant. In total differential of $U(V, N)$ the partial derivative

$$(\partial U/\partial N)_V \equiv \mu_{\text{heat radiation}} = 3.602kT \tag{13}$$

introduces a temperature dependence of chemical potential of heat radiation (Laptev, 2008, 2010). The function $U(S, V, N)$ is an exception and is not a characteristic one because of the relationship (12).

The Sun is a total radiator with the temperature T_S = 5800 K. According to (13), the chemical potential of solar radiation is $3.602kT$ = 173.7 kJ/mol. Then the difference $f(T) = \mu_m - \mu_S$ is a function of the matter temperature T_m. For example, $f(T)$ = –165.0 kJ/mol when T_m = 298.15 K, and it is zero when $T_m = T_S$. According to (13), the function $f(T)$ can be presented as proportional to the dimensionless factor:

$$f(T) = \mu_m - \mu_S = -\mu_S\,(1 - T_m/T_S).$$

According to the Carnot theorem, this factor coincides with the efficiency of the Carnot engine $\eta_C(T_m, T_S)$. Then the function

$$f(T)/\,\mu_S = -\eta_c\,(T_m, T_S) \tag{14}$$

can characterize an efficiency of the idealized Carnot engine-reactor in known limit temperatures T_m and T_S.

In the heat engine there is no process converting heat into work without other changes, i.e. without compensation. The energy accepted by the heat receiver has the function of compensation. If the working body in the heat engine is a heat radiation with the limit temperatures T_m and T_S, then the compensation is presented by the radiation with temperature T_m which is irradiated by the product P at the moment of its formation. We will call this radiation a compensation one in order to make a difference between this radiation and heat radiation of matter.

The efficiency of heat engines with working body consisting of matter and radiation is considered for the first time in (Laptev, 2008, 2010). During the cycle of such an engine–reactor the radiation is cooled from the temperature T_S down to T_m, causing chemical changes in the working body. The working bodies with stored energy or the compensational radiation are exported from the engine at the temperature T_m. The efficiency of this heat engine is the base of the thermodynamic scale of solar radiation chemical action on the working body.

Assume that the reactant R at 298.15 K and solar radiation S with temperature 5800 K are imported in the idealized engine–reactor. The product P, which is saving and transporting stored radiant energy, is exported from the engine at 298.15 K. Limit working temperatures of such an engine are 298.15 K and 5800 K. Then, according to relationships (10), (11), (14), the equation

$$(\mu_m - \mu_S) / \mu_S = -\eta_c (T_m, T_S) \tag{15}$$

defines conditions of maintaining the chemical reaction at steady process at temperature Tm in the idealized Carnot engine–reactor.

According to the Carnot theorem, the way working body receives energy, as well as the nature of the working body do not influence the efficiency of the heat engine. The efficiency remains the same under contact heat exchange between the same limit temperatures. The efficiency of such an idealized engine is

$$\eta_0 (T_m, T_S) = (1 - T_m/T_S). \tag{16}$$

Then the ratio of the values η_C and η_0 from (15), (16)

$$\zeta = \eta_c / \eta_0 = (\mu_P - \mu_R) / [\mu_S (1 - T_m/T_S)]. \tag{17}$$

is a thermodynamic efficiency ζ of chemical action of solar radiation on the working body in the idealized engine–reactor.

We compare efficiencies ζ of the action of solar radiation on water in the working cycle of the idealized engine-reactor if the water at 298.15 K undergoes the following changes:

$$H_2O_{water} + S_{solar\ rad.} = H_2O_{vapor} + M_{heat\ rad.,.vapor}\ ; \tag{18}$$

$$H_2O_{water} + S_{solar\ rad.} = H_{2gas} + \tfrac{1}{2}O_{2gas} + M_{heat\ rad.,}\ H_2 + \tfrac{1}{2}M_{heat\ rad.,}O_2; \tag{19}$$

$$H_2O_{water} + S_{solar\ rad.} = H^+_{gas} + OH^-_{gas} + M_{heat\ rad.,}\ H^+ + M_{heat\ rad.,}\ OH^-. \tag{20}$$

Chemical potentials of pure substances are equal to the Gibbs energies (Yungman & Glushko, 1999). In accordance with (17),

$$\zeta_{(18)} = [-228.61-(-237.25)] / 173.7 / 0.95 = 0.052$$

$$\zeta_{(19)} = \zeta_{(18)} [0 + \tfrac{1}{2} \cdot 0 - (-228.61)] / 173.7 / 0.95 = 0.052\text{x}1.39 = 0.072$$

$$\zeta_{(20)} = \zeta_{(18)} [1517.0 - 129.39 - (-228.61)] / 173.7 / 0.95 = 0.052\text{x}\ 9.79 = 0.51$$

So, in the engine–reactor the reaction (20) may serve as the most effective mechanism of conversion of solar energy.

In the real solar chemical reactors the equilibrium between a matter and radiation is not achieved. In this case the driving force of the chemical process in the reactor at the temperature T will be smaller than the difference of Gibbs energies

$$\Delta G_T = (\mu_P - \mu_R) + (\mu_m - \mu_S). \quad (21)$$

For example, water evaporation at 298.15 K under solar irradiation is caused by the difference of the Gibbs energies

$$\Delta G_{298.15} = -228.61 - (-237.25) + (-165.0) = -156.4 \text{ kJ/mol}.$$

At the standard state (without solar irradiation)

$$\Delta G^0_{298.15} = (\mu_P - \mu_R) = -228.61 - (-237.25) = 8.64 \text{ kJ/mol}.$$

The changes of the Gibbs energies calculated above have various signs: $\Delta G_{298.15} < 0$ and $\Delta G^0_{298.15} > 0$. It means that water evaporation at 298.15 K is possible only with participation of solar radiation. The efficiency ζ of the solar vapor engine will not exceed $\zeta_{(18)} = 5.2\%$. There is no commercial advantage because the efficiency of the conventional vapor engines is higher. However, the efficiency of the solar engine may be higher than that of the vapor one if the condition $\Delta G_{298.15} < 0$ and $\Delta G^0_{298.15} > 0$ is fulfilled. The plant cell where photosynthesis takes place is an illustrative example.

If the condition is $\Delta G_{298.15} < 0$ and $\Delta G^0_{298.15} < 0$ the radiant heat exchange replaces the chemical action of solar radiation. If $\Delta G_{298.15} > 0$ and $\Delta G^0_{298.15} > 0$, then neither radiant heat exchange, nor chemical conversion of solar energy cause any chemical changes in the system at this temperature. The processes (19) and (20) are demonstrative. Nevertheless, at the temperatures when ΔG becomes negative, the chemical changes will occur in the reaction mixture. So, in solar engines–reactors there is a lower limit of the temperature T_m. For example, in (Steinfeld & Palumbo, 2001) it is reported that chemical reactors with solar radiation concentrators have the minimum optimal temperature 1150 K.

The functions $\Delta G(T)$ and $\zeta(T)$ describe various features of the chemical conversion of solar energy. As an illustration we consider the case when the phases R and P are in thermodynamic equilibrium. For example, the chemical potentials of the boiling water and the saturated vapor are equal. Then both their difference $(\mu_P - \mu_R)$ and the efficiency ζ of the chemical action of solar radiation are zero, althought it follows from Eq. (21) that $\Delta G(T) < 0$. Without solar irradiation the equation $\Delta G(T) = 0$ determines the condition of the thermodynamic equilibrium, and the function $\zeta(T)$ loses its sense.

The thermodynamic scale of efficiency $\zeta(T)$ of the chemical action of solar radiation presented in this paper is a necessary tool for choice of optimal design of the solar engines_reactors. It is simple for application while its values are calculated from the experimentally obtained data of chemical potentials and temperature. Varying the values of chemical potentials and temperature makes it possible to model (with help of expressions (17), (21)) the properties of the working body, its thermodynamic state and optimal conditions for chemical changes in solar engines and reactors in order to bring commercial advantages of alternative energy sources.

6. Thermodynamic efficiency of the photosynthesis in plant cell

It is known that solar energy for glucose synthesis is transmitted as work (Berg et al., 2010; Lehninger et al., 2008; Voet et al., 2008; Raven et al., 1999). Here it is shown for the first time that there are pigments which reemit solar photons whithout energy conversion in form of heat dissipation and work production. We found that this antenna pigments make 77% of all

pigment molecula in a photosystem. Their existance and participation in energy transfer allow chloroplasts to overcome the efficiency threshold for working pigments as classic heat engine and reach 71% efficiency for light and dark photosynthesis reactions. Formula for efficiency calculation take into account differences of photosynthesis in specific cells. We are also able to find the efficiency of glycolysis, Calvin and Krebs cycles in different organisms.

The Sun supplies plants with energy. Only 0.001 of the solar energy reaching the Earth surface is used for photosynthesis (Nelson & Cox, 2008; Pechurkin, 1988) producing about 1014 kg of green plant mass per year (Odum, 1983). Photosynthesis is thought to be a low–effective process (Ivanov, 2008). The limiting efficiency of green plant is defined to be 5% as a ratio of the absorbed solar energy and energy of photosynthesis products (Odum,1983; Ivanov, 2008). Here is shown that the photosynthesis efficiency is significantly higher (71% instead of 5%) and it is calculated as the Carnot efficiency of the solar engine_reactor with radiation and matter as a single working body.

The photosynthesis takes place in the chloroplasts containing enclosed stroma, a concentrated solution of enzymes. Here occure the dark reactions of the photosynthesis of glucose and other substances from water and carbon dioxide. The chlorophyll traps the solar photon in photosynthesis membranes. The single membrane forms a disklike sac, or a thylakoid. It encloses the lumen, the fluid where the light reactions take place. The thylakoids are forming granum (Voet et al., 2008; Berg et al., 2010). Stacks of grana are immersed into the stroma.

When solar radiation with the temperature T_S is cooled in the thylakoid down to the temperature T_A, the amount of evolved radiant heat is a fraction

$$\eta_U = 1 - (T_A/T_S)^4$$

of the energy of incident solar radiation (Wuerfel, 2005). The value η_U is considered here as an efficiency of radiant heat exchange between the black body and solar radiation (Laptev, 2006).

Tylakoids and grana as objects of intensive radiant heat exchange have a higher temperature than the stroma. Assume the lumen in the tylakoid has the temperature T_A = 300 K and the stroma, inner and outer membranes of the chloroplast have the temperature T_0 = 298 K. The solar radiation temperature T_S equals to 5800 K.

The limiting temperatures T_0, T_A in the chloroplast and temperature T_S of solar radiation allow to imagine a heat engine performing work of synthesis, transport and accumulation of substances. In idealized Carnot case solar radiation performs work in tylakoid with efficiency

$$\eta_C = 1 - T_A/T_S = 0.948,$$

and the matter in the stroma performs work with an efficiency

$$\eta_0 = 1 - T_0/T_A = 0.0067.$$

The efficiency $\eta_0\eta_C$ of these imagined engines is 0.00635.

The product $\eta_0\eta_C$ equals to the sum $\eta_0 + \eta_C - \eta_{0S}$ (Laptev, 2006). Value η_{0S} is the efficiency of Carnot cycle where the isotherm T_S relates to the radiation, and the isotherm T_0 relates to the matter. The values η_{0S} and η_C are practically the same for chosen temperatures and $\eta_{0S}/\eta_0\eta_C$ = 150. It means that the engine where matter and radiation performing work are a single working body has 150 times higher efficiency than the chain of two engines where matter and radiation perform work separately.

It is known (Laptev, 2009) that in the idealized Carnot solar engine–reactor solar radiation S produces at the temperature TA a chemical action on the reagent R

$$\mathbf{R}_{\text{reagent}} + \mathbf{S}_{\text{solar radiation}} \leftrightarrow \mathbf{P}_{\text{product}} + \mathbf{M}_{\text{thermal radiation of product}}$$

with efficiency

$$\zeta = (\mu_P - \mu_R)/[\mu_S/(1 - T_A/T_S)], \tag{22}$$

where μ_P, μ_R are chemical potentials of the substances, μ_S is the chemical potential of solar radiation equal to $3.602kT_S$ = 173.7 kJ/mol. The efficiency of use of water for alternative fuel synthesis is calculated in (Laptev, 2009).

Water is a participant of metabolism. It is produced during the synthesis of adenosine triphosphate (ATP) from the adenosine diphosphate (ADP) and the orthophosphate (P_i)

$$ADP + P_i = ATP + H_2O. \tag{23}$$

Water is consumed during the synthesis of the reduced form of the nicotinamide adenine dinucleotide phosphate (NADPH) from its oxidized form ($NADP^+$)

$$2NADP^+ + 2H_2O = 2NADPH + O_2 + 2H^+_{\text{thylakoid}} \tag{24}$$

and during the glucose synthesis

$$6CO2 + 6H_2O = C_6H_{12}O_6 + 6O_2. \tag{25}$$

Changes of the Gibbs energies or chemical potentials of substances in the reactions (23)–(25) are 30.5, 438 and 2850 kJ/mol, respectively (Voet et al., 2008).

The photosynthesis is an example of joint chemical action of matter and radiation in the cycle of the idealized engine–reactor, when the water molecule undergoes the changes according to the reactions (23)–(25). According to (22), the photosynthesis efficiency ζ_{Ph} in this model is

$$\zeta_{(5)} \times 1/2\zeta_{(6)} \times 1/6\zeta_{(7)} = 71\%.$$

The efficiency ζ_{Ph} is smaller than the Landsberg limiting efficiency

$$\eta_L = \eta_U - 4T_0/3T_S + 4T_0\,T_A^3/3\,T_S^4, \tag{26}$$

known in the solar cell theory (Wuerfel, 2005) as the efficiency of the joint chemical action of the radiation and matter per cycle. ζ_{Ph} and the temperature dependence η_L are shown in Fig. 12 by the point F and the curve LB respectively. They are compared with the temperature dependence of efficiencies $\eta_0\eta_C\eta_U$ (curve CB) and $\eta_{0S}\eta_U$ (curve KB). Value η_U is close to unity because $(T_A/T_S)^4 \sim 10^{-5}$.

We draw in Fig. 12 an isotherm t–t' of η values for T_A = 300 K. It is found that η_{0S} = 94.8% at the interception point K, η_L = 93.2% at the point L and $\eta_0\eta_C\eta_U$ = 0.635% at the point C. The following question arises: which processes give the chloroplasts energy for overcoming the point C and achieving an efficiency ζ_{Ph} = 71% at the point F?

First of all one should note that the conversion of solar energy into heat in grana has an efficiency η_g smaller than η_U of the radiant heat exchange for black bodies. From (26) follows that the efficiency ζ_{Ph} cannot reach the value η_L due to necessary condition $\eta_g < \eta_U$.

Besides in the thylakoid membrane the photon reemissions take place without heat dissipation (Voet et al., 2008; Berg et al., 2010). The efficiency area between the curves *LB* and *CB* relates to photon reemissions or antenna processes. They can be reversible and irreversible. The efficiencies of reversible and irreversible processes are different. Then the point *F* in the isotherm *t*–*t*' is the efficiency of engine with the reversible and irreversible antenna cycles.

The antenna process performs the solar photon energy transfer into reaction centre of the photosystem. Their illustration is given in (Voet et al., 2008; Berg et al., 2010). Every photosystem fixes from 250 to 400 pigments around the reaction center (Raven et al., 1999). In our opinion a single pigment performs reversible or irreversible antenna cycles. The antenna cycles form antenna process. How many pigments make the reversible process in the photosynthetic antenna complex?

One can calculate the fraction of pigments performing the reversible antenna process if the line *L*C in Fig. 12 is supposed to have the value equal unity. In this case the point *F* corresponds to a value $x = \zeta/(\eta_L - \eta_0\eta_C\eta_U) = 0.167$. This means that 76.7% of pigments make the revesible antenna process. 23.3% of remaining pigments make an irreversible energy transfer between the pigments to the reaction centres. The radiant excitation of electron in photosystem occurs as follows:

$$\text{chlorophyll } a + \text{photon} \leftrightarrow \text{chlorophyll } a^{+} + e^{-}. \tag{27}$$

The analogous photon absorption takes place also in the chlorophylls *b*, *c*, *d*, various carotenes and xanthophylls contained in different photosystems (Voet et al., 2008; Berg et al., 2010). The excitation of an electron in the photosystems P680 and P700 are used here as illustrations of the reversible and irreversible antenna processes.

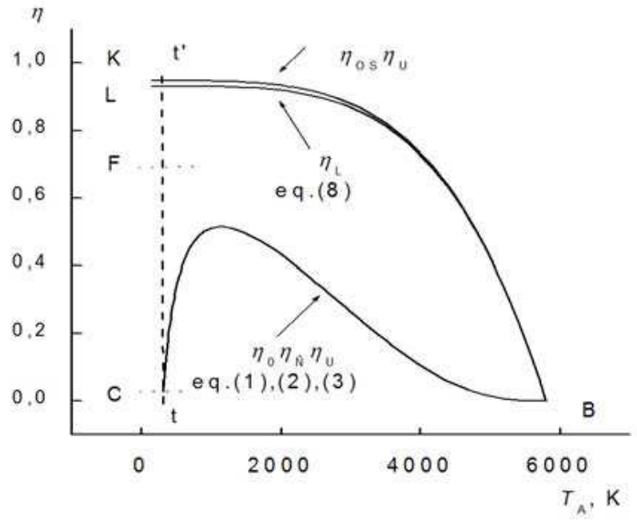

Fig. 12. The curve *CB* is the efficiency of the two Carnot engines (Laptev, 2005). The curve *LB* is the efficiency of the reversible heat engine in which solar radiation performs work in combination with a substance (Wuerfel, 2005). The curve *KB* is the efficiency of the Carnot solar engine_reactor (Laptev, 2006), multiplied by the efficiency η_U of the heat exchange between black bodies. The isotherm *t*–*t*' corresponds to the temperature 300 K. The calculated photosynthesis efficiency is presented by the point *F* in the isotherm.

Schemes of working and antenna cycles are shown in Fig. 13. Working pigment (a) is excited by the photon in the transition 1 → 3. Transition 3 → 2 corresponds to the heat compensation in the chloroplast as engine–reactor. The evolved energy during the transition 2 → 1 is converted into the work of electron transfer or ATP and NADPH synthesis.
When the antenna process passes beside the reaction centre, the photosystems make the reversible reemissions. Fig. 13 presents an interpretation of absorption and emission of photons in antenna cycles. The reemission 2 → 3 → 2 shows a radiant heat exchange. The reemissions 1 → 2 → 1 and 1 → 3 → 1 take place according to (27). Examples are the pigments in chromoplasts.
According to the thermodynamic postulate, the efficiency of reversible process is limited. In our opinion, just the antenna processes in the pigment molecules of the tylakoid membrane allow the photosystems to overcome the forbidden line (for a heat engine efficiency) *CB* in Fig. 12 and to achieve the efficiency $\zeta_{Ph} = 71\%$ in the light and dark photosynthesis reactions.
There are no difficulties in taking into account in (22) the features of the photosynthesis in different cells. The efficiency of glycolyse, Calvin and Krebs cycles in various living structures may be calculated by the substitution of solar radiation chemical potential in the expression (22) by the change of chemical potentials of substances in the chemical reaction.
The cell is considered in biology as a biochemical engine. Chemistry and physics know attempts to present the plant photosynthesis as a working cycle of a solar heat engine (Landsberg, 1977). The physical action of solar radiation on the matter of nonliving systems during antenna and working cycles of the heat engine is described in (Laptev, 2005, 2008). In this article the Carnot theorem has been used for calculation of the thermodynamic efficiency of the photosynthesis in plants; it is found that the efficiency is 71%.

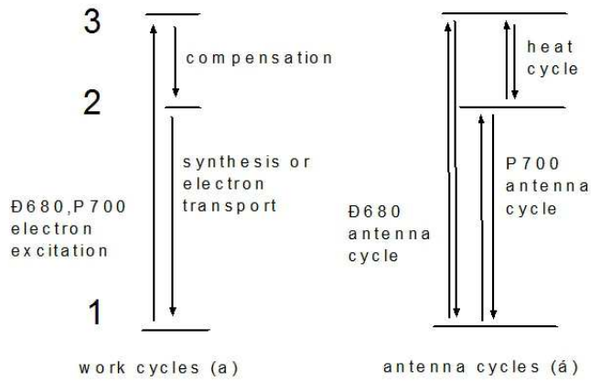

Fig. 13. The interpretation of energy transitions in the work (a) and antenna (b) cycles. Level *1* shows the ground states, levels *2*, *3* present excited states of pigment molecules.

One can hope that the thermodynamic comparison of antenna and working states of pigments in the chloroplast made in this work will open new ways for improving technologies of solar cells and synthesis of alternative energy sources from the plant material.

7. Condensate of thermal radiation

Thermal radiation is a unique thermodynamic system while the expression $dU=TdS-pdV$ for internal energy U, entropy S, and volume V holds the properties of the fundamental

equation of thermodynamics regardless the variation of the photon number (Kondepudi & Prigogin, 1998. Bazarov, 1964). Differential expression $\mathrm{d}p/\mathrm{d}T=S/V$ for pressure p and temperature T is valid for one-component system under phase equilibrium if the pressure does not depend on volume V (Muenster, 1970). Thermal radiation satisfies these conditions but shows no phase equilibrium.

The determinant of the stability of equilibrium radiation is zero (Semenchenko, 1966). While the „zero" determinants are related to the limit of stability, there are no thermodynamic restrictions for phase equilibrium of radiation (Muenster, 1970). However, successful attempts of finding thermal radiation condensate in any form are unknown. This work aims to support enthusiasm of experimental physicists and reports for the first time the phenomenological study of the thermodynamic medium consisting of radiation and condensate.

It is known (Kondepudi & Prigogin, 1998; Bazarov, 1964), that evolution of radiation is impossible without participating matter and it realizes with absorption, emission and scattering of the beams as well as with the gravitational interaction. Transfer of radiation and electron plasma to the equilibrium state is described by the kinetic equation. Some of its solutions are treated as effect of accumulation in low-frequency spectrum of radiation, as Bose-condensation or non-degenerated state of radiation (Kompaneets, 1957; Dreicer, 1964; Weymann, 1965; Zel'dovich & Syunyaev, 1972; Dubinov A.E. 2009). A known hypothesis about Bose-condensation of relic radiation and condensate evaporation has a condition: the rest mass of photon is thought to be non-zero (Kuz'min & Shaposhnikov, 1978). Nevertheless, experiments show that photons have no rest mass (Spavieri & Rodrigues, 2007).

Radiation, matter and condensate may form a total thermal equilibrium. According to the transitivity principle of thermodynamic equilibrium (Kondepudi & Prigogin, 1998; Bazarov, 1964), participating condensate does not destroy the equilibrium between radiation and matter. Suppose that matter is a thermostat for the medium consisting of radiation and condensate. A general condition of thermodynamic equilibrium is an equality to zero of virtual entropy changes δS or virtual changes of the internal energy δU for media (Bazarov, 1964; Muenster, 1970; Semenchenko, 1966). Using indices for describing its properties, we write $S=S_{\mathrm{rad}}+S_{\mathrm{cond}}$, $U=U_{\mathrm{rad}}+U_{\mathrm{cond}}$. The equilibrium conditions $\delta S_{\mathrm{rad}}+\delta S_{\mathrm{cond}}=0$, $\delta U_{\mathrm{rad}}+\delta U_{\mathrm{cond}}=0$ will be completed by the expression $T\delta S=\delta U+p\delta V$, and then we get an equation

$$(1/T_{\mathrm{cond}}-1/T_{\mathrm{rad}})\delta U_{\mathrm{cond}}+(p_{\mathrm{cond}}/T_{\mathrm{cond}})\delta V_{\mathrm{cond}}+(p_{\mathrm{rad}}/T_{\mathrm{rad}})\delta V_{\mathrm{rad}}=0.$$

If $V_{\mathrm{rad}}+V_{\mathrm{cond}}=V=\mathrm{const}$ and $\delta V_{\mathrm{rad}}=-\delta V_{\mathrm{cond}}$, then for any values of variations δU_{cond} and δV_{cond} we find the equilibrium conditions: $T_{\mathrm{rad}}=T_{\mathrm{cond}}=T$ and $p_{\mathrm{rad}}=p_{\mathrm{cond}}=p$. When condensate is absolutely transparent for radiation, it is integrated in condensate, so that $V_{\mathrm{rad}}=V_{\mathrm{cond}}=V$ and $\delta V_{\mathrm{rad}}=\delta V_{\mathrm{cond}}$. Thus, conditions

$$T_{\mathrm{rad}}=T_{\mathrm{cond}},\qquad p_{\mathrm{rad}}=-p_{\mathrm{cond}} \tag{28}$$

are satisfied for any values of variations δU_{cond} and δV_{cond}.

The negative pressure arises in cases, when $U-TS+pV=0$ and $U>TS$. We ascribe these expressions to the condensate and assume the existence of the primary medium, for which the expression $S_0=S_{\mathrm{cond}}+S_{\mathrm{rad}}$ is valid in the same volume. Now we try to answer the question about the medium composition to form the condensate and radiation from indefinitely small local perturbations of entropy S_0 of the medium. Two cases have to be examined.

Suppose that the primary medium is radiation and for this medium $U_{00,\mathrm{rad}}-TS_0+p_{\mathrm{rad}}V=0$. Then the condition $U_{00,\mathrm{rad}}<U_{\mathrm{rad}}+U_{\mathrm{cond}}$ is satisfied for values of p and T necessary for equilibrium. According to this inequality and the Gibbs stability criterion (Muenster, 1970), the medium consisting of the condensate and radiation is stable relatively to primary radiation, i.e. the condensation of primary radiation is a forced process.

In contrary, the equilibrium state of condensate and radiation arises spontaneously from the primary condensate, because $U_{00,\mathrm{cond}}>U_{\mathrm{rad}}+U_{\mathrm{cond}}$, if $U_{00,\mathrm{cond}}-TS_0+p_{\mathrm{cond}}V=0$. However, the condensate has to lower its energy before the moment of the equilibrium appearance to prevent self-evaporation of medium into radiation. Such a process is possible under any infinitely small local perturbations of the entropy S_0. Really, the state of any equilibrium system is defined by the temperature T and external parameters (Kondepudi & Prigogin, 1998; Bazarov, 1964; Muenster, 1970).

While the state of investigated medium is defined by the temperature only, the supposed absence of external forces allows the primary condensate to perform spontaneous adiabatic extension with lowering energy by factor $\Delta U_{\mathrm{cond}}=U_{0,\mathrm{cond}}-U_{00,\mathrm{cond}}=p_{\mathrm{cond}}\Delta V$. When the energy rest will fulfill the condition $U_{0,\mathrm{cond}}=U_{\mathrm{rad}}+U_{\mathrm{cond}}$, the required condition $U_{0,\mathrm{cond}}-TS_0+p_{\mathrm{cond}}V=0$ for arising equilibrium between condensate and radiation will be achieved.

Let's consider the evolution of the condensate being in equilibrium with radiation. Once the medium is appeared, this medium consisting of the equilibrium condensate and radiation can continue the inertial adiabatic extension due to the assumed absence of external forces. When $V_{\mathrm{rad}}\equiv V_{\mathrm{cond}}$, the second law of thermodynamics can be written as $u=Ts-p$, where u and s are densities of energy and entropy, respectively. Fig. 14 plots a curve of radiation extension as a cubic parabola $s_{\mathrm{rad}}=4\sigma T^3/3$, where σ is the Stefan-Boltzmann constant. Despite the fact that the density of entropy of the condensate is unknown, we can show it in Fig.1 as a set of positive numbers $\lambda=Ts$, if each λ_i is ascribed an equilateral hyperbola $s_{\mathrm{cond}}=\lambda_i/T$. Fig.14 illustrates both curves.

We include the cross-section point c_i of the hyperbola cd and the cubic parabola ab in Fig. 14 in the interval $[c_0, c_k]$. Assume the generation of entropy along the line cd outside this interval and the limits of the interval are fixing the boundary of the medium stability. Absence of the entropy generation inside the interval $[c_0, c_k]$ means that the product $2s_i(T_k-T_0)$ is $\int_{T_0}^{T_k} \mathrm{d}T(s_{\mathrm{cond}}+s_{\mathrm{rad}})$. By substituting s we can see that these equalities are valid only at $T_0=T_k=T_i$. So, if the condensate and radiation are in equilibrium, the equality $s_{\mathrm{cond}}=s_{\mathrm{rad}}$ is also valid.

Thus, when the equilibrium state is achieved the medium extension is realized along the cross-section line of the parabola and hyperbolas. Equalities $s_{\mathrm{cond}}=s_{\mathrm{rad}}=4\sigma T^3/3$ are of fundamental character; all other thermodynamic values for the condensate can be derived from these values. For example, we find that $\lambda_i=4\sigma T_i^4/3$. For the condensate $u-Ts+p=0$ is valid. Then, according to (28),

$$u_{\mathrm{cond}}=Ts-p_{\mathrm{cond}}=5\sigma T^4/3. \tag{29}$$

For the equilibrium medium consisting of the condensate and radiation $u_{\mathrm{cond}}=5u_{\mathrm{rad}}/3$ and $u_0=u_{\mathrm{rad}}+u_{\mathrm{cond}}=8\sigma T^4/3=2\lambda$. For the primary condensate before its extension $u_{00}=u_{\mathrm{rad}}+u_{\mathrm{cond}}-p=3\sigma T^4$. For thermal radiation $u_{\mathrm{rad}}=3p$ and the pressure is always positive (Kondepudi & Prigogin, 1998; Bazarov, 1964).

The extension of the medium is an inerial process, so that the positive pressure of radiation p_{rad} lowers, and the negative pressure of the condensate p_{cond} increases according to the condition (1). Matter is extended with the medium. As it is known in cosmological theory (Kondepudi & Prigogin, 1998; Bazarov, 1964), the plasma inertial extension had led to formation of atoms and distortion of the radiation-matter equilibrium. Further local unhomogeneities of matter were appeared as origins of additional radiation and, consequently, matter created a radiation excess in the medium after the equilibrium radiation-matter was disturbed This work supposes that radiation excess may cause equilibrium displacement for the medium, thus radiation and condensate will continue extending inertially in a non-equilibrium process.

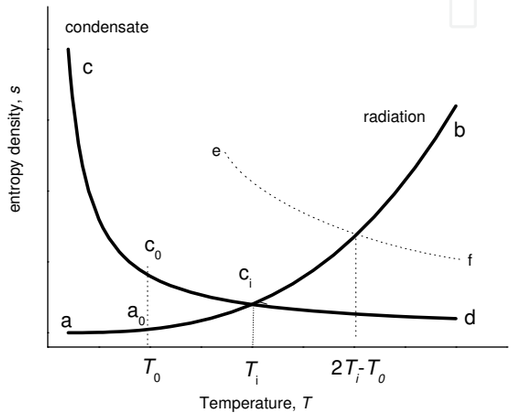

Fig. 14. Schematically plots the density of entropy for radiation (curve *ab*) and for a condensate (curves *cd* and *ef*). The positive pressure of the radiation and negative pressure of condensate are equal by absolute value at the points c_i and e_k at the interceptions of these curves.

We assume that the distortion of the equilibrium radiation-condensate had been occurred at the temperature T_i of the medium at the point c_i in Fig. 14. The radiation will be extended adiabatically along the line $c_i a$ of the cubic parabola without entropy generation. While the condition $V_{rad}=V_{cond}$ is satisfied if the equilibrium is disturbed, the equality $s_{cond}=s_{rad}$ points out directions of the condensate extension without entropy generation. As it is shown in Fig.14, the unchangeable adiabatic isolation is possible if the condensate extends along the isotherm T_i without heat exchange with radiation. Differentiation of the expression $U_{cond}-T_iS_{cond}+p_{cond}V=0$ with T=const and S=const gives that p_{cond} is also constant.

The medium as a whole extends in such a manner that the positive pressure p_{rad} of radiation decreases, and the negative pressure p^*_{cond} remains constant. As radiation cools down, the ratio p^*/p_{rad} lowers, the dominant p^* of the negative pressure arises, and the medium begins to extend with positive acceleration.

The thermodynamics defines energy with precision of additive constant. If we assume this constant to be equal to TS_{cond}, then the equality $u^*_{cond}=U^*_{cond}/V = -p^*_{cond}$, is valid; this equality points out the fixed energy density of the condensate under its expansion after distortion of the medium equilibrium.

The space is transparent for relic radiation which is cooling down continuously under adiabatic extension of the Universe. Assuming existence of the condensate of relic radiation we derive an expression for a fixed energy density of the condensate u^* with the beginning of accelerated extension of the Universe. The adiabatic medium with negative pressure and

a fixed energy density 4 GeV/m³ is supposed to be the origin of the cosmological acceleration. The nature of this phenomenon is unknown (Chernin, 2008; Lukash & Rubakov, 2008; Green, 2004) . What part of this energy can have a relic condensate accounting the identical equation of state $u = -p$ for both media?

The relic condensate according to (29) has the energy density 4 GeV/m³ when the temperature of relic radiation is about 27 K. If the accelerated extension of the cosmological medium arises at $T^* \leq 27$ K, the part of energy of the relic condensate in the total energy of the cosmological medium is $(T^*/27)^4$. According to the Fridman model T^* corresponds to the red shift ≈0.7 (Chernin, 2008) and temperature 4.6 K. Then the relic condensate can have a 0.1% part of the cosmological medium.

As a conclusion one should note that the negative pressure of the condensate of thermal radiation is Pascal-like and isotropic, it is constant from the moment as the equilibrium with radiation was disturbed by the condensate and is equal (by absolute value) to the energy density with precision of additive constant. The condensate of thermal radiation is a physical medium which interacts only with the radiation and this physical medium penetrates the space as a whole. This physical medium cannot be obtained under laboratory conditions because there are always external forces for a thermodynamic system in laboratory. While this paper was finalized the information (Klaers et al., 2009) showed the photon Bose-condensate can be obtained. This condensate has no negative pressure while it is localized in space. It seems very interesting to find in the nature a condensate of thermal radiation with negative pressure. Possible forms of physical medium with negative pressure and their appearance at cosmological observations are widely discussed. The radiation can consist of other particles, then the photon, among them may be also unknown particles. We hope that modelling the medium from the condensate and radiation will be useful for checking the hypotheses and will allow explaining the nature of the substance responsible for accelerated extension of the Universe. The medium from thermal radiation and condensate is the first indication of the existence of physical vacuum as one of the subjects in classical thermodynamics and the complicated structure of the dark energy.

8. Electrical properties of copper clusters in porous silver of silicon solar cells

Technologies for producing electric contacts on the illuminated side of solar cells are based on chemical processes. Silver technologies are widely used for manufacturing crystalline silicon solar cells. The role of small particles in solar cells was described previously (Hitz, 2007; Pillai, 2007; Han, 2007; Johnson, 2007). The introduction of nanoparticles into pores of photon absorbers increases their efficiency. In our experiments copper microclusters were chemically introduced into pores of a silver contact. They changed the electrical properties of the contact: dark current, which is unknown for metals, was detected.

In the experiments, we used 125 x×125-mm commercial crystalline silicon wafers Si<P>/SiN_x (70 nm)/Si<B> with a silver contact on the illuminated side. The silver contact was porous silver strips 10–20 μm thick and 120–130 μm wide on the silicon surface. The diameter of pores in a contact strip reached 1μm. The initial material of the contact was a silver paste (Dupont), which was applied to the silicon surface through a tungsten screen mask. After drying, organic components of the paste were burned out in an inert atmosphere at 820–960° C. Simultaneously, silver was burned in into silicon through a 70-nm-thick silicon nitride layer. After cooling in air, the wafer was immersed in a copper salt

solution under the action of an external potential difference; then, the wafer was washed with distilled water and dried with compressed nitrogen until visible removal of water from the surface of the solar cell (Laptev & Khlyap, 2008).

The crystal structure of the metal phases was studied by grazing incidence X-ray diffraction. A 1-μm-thick copper layer on the silver surface has a face-centered cubic lattice with space group *Fm*3*m*. The morphology of the surface of the solar cell and the contact strips before and after copper deposition was investigated with a KEYENCE-5000 3D optical microscope. Fig. 15 presents the result of computer processing of images of layer-by-layer optical scanning of the surface after copper deposition.

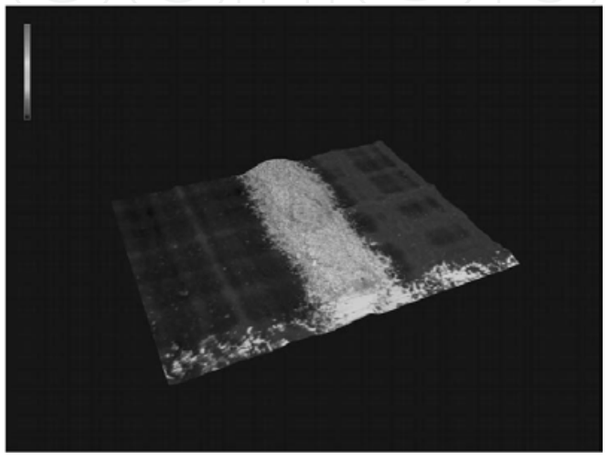

Fig. 15. Contact strip morphology. Scanning area 430 x 580 μm²; magnification 5000x.

The copper deposition onto the silver strips did not change the shape and profile of the contact, which was a regular sequence of bulges and compressions of the contact strip. The differences in height and width reached 5 μm. In some cases, thin copper layers caused slight compression of the contact in height. The profiles of the contacts were studied using computer programs of the optical microscope. It was found that copper layers to 1 μm in thickness on the silver contact could cause a decrease in the strip height by up to 10%.

The chemical composition of the contact and the depth distribution of copper were investigated by energy dispersive X-ray analysis, secondary ion mass spectrometry, and X-ray photoelectron spectroscopy. The amount of copper in silver pores was found to decrease with depth in the contact. Copper was found at the silicon–silver interface. No copper diffusion into silicon was detected.

The resistivity of the contacts was measured at room temperature with a Keithley 236 source-measure unit. Two measuring probes were placed on the contact strips at a distance of 8 mm from each other. A probe was a tungsten needle with a tip diameter of 120 μm. The measurements were made on two samples in a box with black walls and a sunlight simulator. Fig. 16 presents the results of the experiments.

Line *1* is the current–voltage diagram for the initial silver contact strip on the silicon wafer surface. The other lines are the current–voltage diagrams for the contacts after copper deposition. All the lines confirm the metallic conductance of the contact strips. The current–voltage diagrams for the contacts with copper clusters differ by the fact that they do not pass through the origin of coordinates for both forward and reverse currents. A current through a metal in the absence of an external electric field is has not been observed. In our

experiment, the light currents were 450 μA in the contact where copper clusters were only in silver pores and 900 μA in the contact where copper clusters were both in silver pores and on the silver surface.

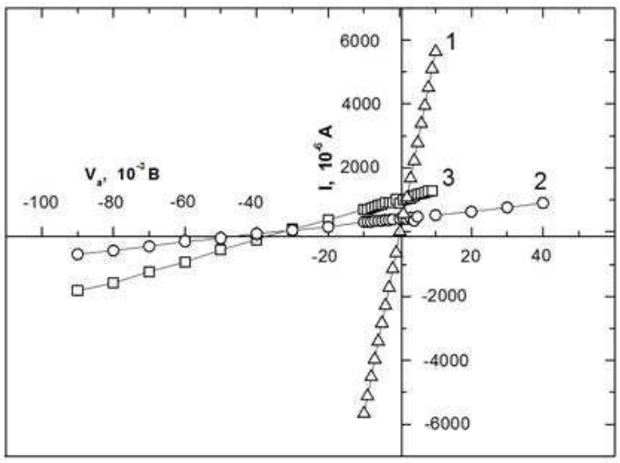

Fig. 16. Electrical properties of (*1*) a silver contact strip, (*2*) a contact strip with copper clusters in silver pores, and (*3*) a strip with a copper layer on the surface and copper clusters in silver pores.

It is worth noting that the electric current in the absence of an external electric field continued to flow through these samples after the sunlight simulator was switched off. The light and dark currents in the contact strips are presented in Fig. 17. It is seen that the generation of charge carriers in the dark at zero applied bias is constant throughout the experiment time. The dark current in the silver contact is caused by the charge carrier generation in the contact itself. The source of dark-current charge carriers are copper clusters in silver pores and on the silver surface.

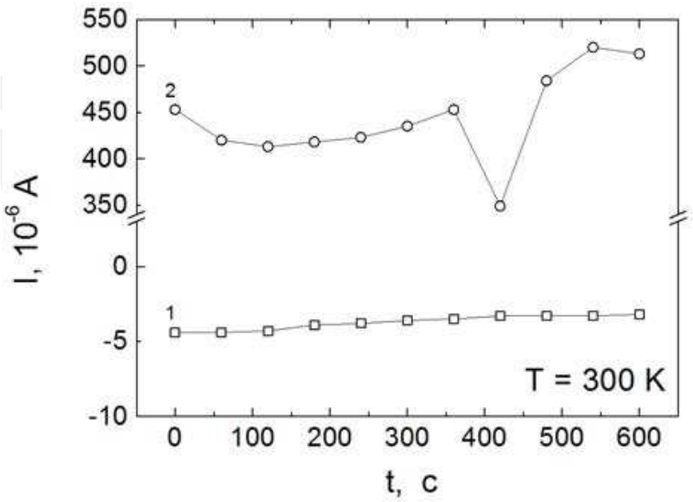

Fig. 17. Time dependence of the (*1*) dark and (*2*) light currents at zero applied bias in contact strips with copper clusters in silver pores.

The current in the silver contact with copper clusters while illuminating the solar cell is caused by the generation of charge carriers in the semiconductor part of the silicon wafer. The number of charge carriers generated in the *p–n* junction is two orders of magnitude larger than the number of charge carriers in copper clusters since the light current is so larger than the dark current (Fig. 17).

The copper deposition onto silver does not lead to the formation of a silver–copper solid solution. The contact of the crystal structures gives rise to an electric potential difference. This is insufficient for generation of current carriers.

However, the contact of the copper and silver crystal structures causes compression of the metal strip and can decrease the metal work function of copper clusters.

We consider that the charge carrier generation in the dark by copper clusters in the contact strip as a component of the solar cell is caused by the deformation of the strip. It is known (Albert & Chudnovsky, 2008), that deformation of metal cluster structures can induce high-temperature superconductivity. Therefore, it is necessary to investigate the behavior of the studied samples in a magnetic field.

Solar energy conversion is widely used in electric power generation. Its efficiency in domestic and industrial plants depends on the quality of components (Slaoui A & Collins, 2007). Discovered in this work, the dark current in the silver contact on the illuminated side of a silicon solar cell generates electricity in amount of up to 5% of the rated value in the absence of sunlight. Therefore, the efficiency of solar energy conversion plants with copper–silver contacts is higher even at the same efficiency of the semiconductor part of the solar cell.

9. Metallic nanocluster contacts for high-effective photovoltaic devices

High efficiency of solar energy conversion is a main challenge of many fields in novel nanotechnologies. Various nanostructures have been proposed early (Pillai et al., 2007; Hun et al., 2007; Johnson et al., 2007; Slaoui & Collins, 2007). However, every active element cannot function without electrodes. Thus, the problem of performing effective contacts is of particular interest.

The unique room-temperature electrical characteristics of the porous metallic nanocluster-based structures deposited by the wet chemical technology on conventional silicon-based solar cells were described in (Laptev & Khlyap, 2008). We have analyzed the current-voltage characteristics of Cu-Ag-metallic nanocluster contact stripes and we have registered for the first time dark currents in metallic structures. Morphological investigations (Laptev & Khlyap, Kozar et al., 2010) demonstrated that copper particles are smaller than 0.1 μm and smaller than the pore diameter in silver.

Electrical measurements were carried out for the nanoclustered Ag/Co-contact stripe (Fig.18, inset) and a metal-insulator-semiconductor (MIS) structure formed by the silicon substrate, SiN_x cove layer, and the nanocluster stripe. Fig. 18 plots experimental room-temperature current-voltage characteristics (IVC) for both cases.

As is seen, the nanocluster metallic contact stripe (function 3 in Fig. 18) demonstrates a current-voltage dependence typical for metals. The MIS-structure (functions 1 and 2 in Fig. 18) shows the IVC with a weak asymmetry at a very low applied voltage; as the external electric field increases, the observed current-voltage dependence transforms in a typical "metallic" IVC. More detailed numerical analysis was carried out under re-building the experimental IVCs in a double-log scale.

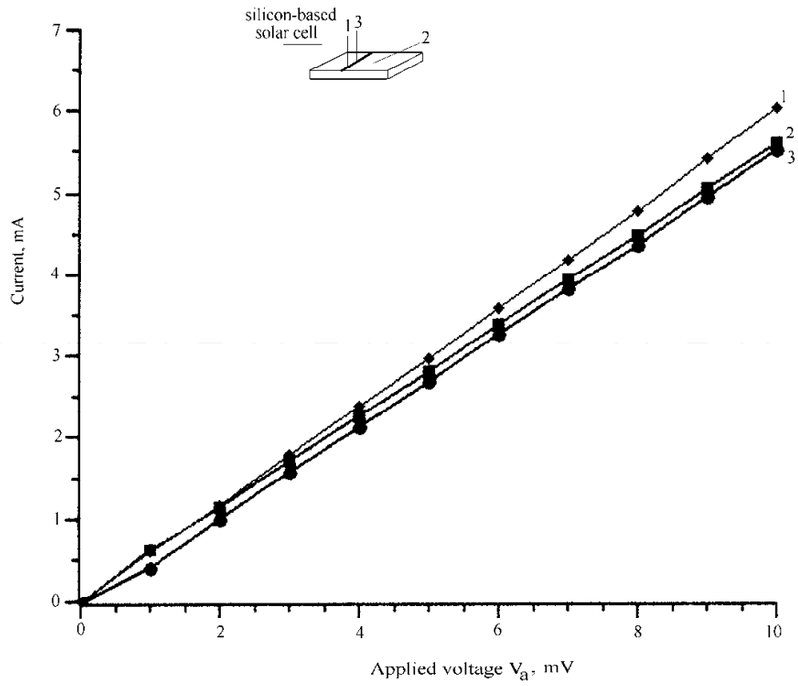

Fig. 18. Room-temperature current-voltage characteristics of the investigated structures <8see text above): functions 1 and 2 are "forward" and "reverse" currents of the MIS-structure (contacts 1-2), and the function 3 is a IVC for the contacts 1-3.

Fig. 19 illustrates a double-log IVCs for the investigated structure. The numerical analysis has shown that both "forward" and 'reverse" currents can be described by the function

$$I = f(V_a)^m,$$

where I is the experimental current (registered under the forward or reverse direction of the applied electric field), and V_a is an applied voltage. The exponential factor *m* changes from 1.7 for the "forward" current at V_a up to 50 mV and then decreases down to ~1.0 as the applied bias increases up to 400 mV; for the "reverse" current the factor *m* is almost constant (~1.0) in the all range of the external electric field.
Thus, these experimental current-voltage characteristics (we have to remember that the investigated structure is a metallic cluster-based quasi-nanowire!) can be described according to the theory (Sze & Ng, 2007) as follows: the first section of forward current

$$I = T_{tun}A_{el}(4\varepsilon/9L^2)(2e/m^*)^{1/2}(V_a)^{3/2}$$

(ballistic mode) and the second one as

$$I = T_{tun}A_{el}(2\varepsilon v_s/L^2)V_a,$$

and the reverse current is

$$I = T_{tun}A_{el}(2\varepsilon v_s/L^2)V_a$$

(velocity saturation mode). Here T_{tun} is a tunneling transparency coefficient of the potential barrier formed by the ultrathin native oxide films, A_{el} and L are the electrical

area and the length of the investigated structure, respectively, ε is the electrical permittivity of the structure, m* is the effective mass of the charge carriers in the metallic Cu-Ag-nanoclucter structure, and v_s is the carrier velocity (Kozar et al., 2010). These experimental data lead to the conclusion that the charge carriers can be ejected from the pores of the Cu-Ag-nanocluster wire in the potential barrier and drift under applied electric field (Sze & Ng, 2007; Peleshchak & Yatsyshyn, 1996; Datta, 2006; Ferry & Goodnick, 2005; Rhoderick, 1978).

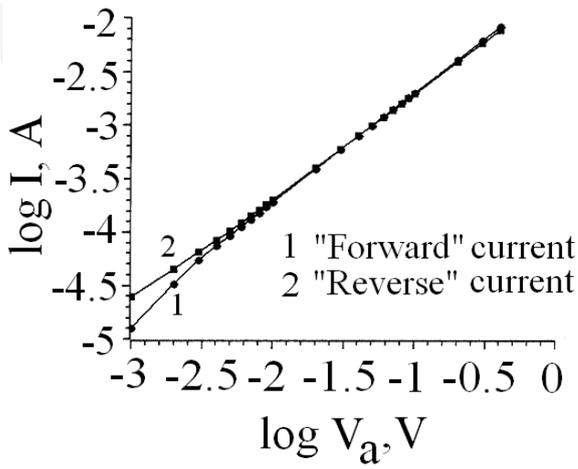

Fig. 19. Experimental room-temperature current-voltage characteristic of the examined structure in double-logarithmic scale.

10. References

Albert J. & Chudnovsky E.M. (2008). Voltage from mechanical stress in type-II superconductors: Depinning of the magnetic flux by moving dislocations, *Appl. Phys. Lett.*, Vol. 93, Issue 4, pp. 042503-1–3, doi:10.1063/1.2960337, 0003-6951(print), 1077-3118 (online).

Badesku V., Landsberg P. T. & De Vos A., Desoete B. (2001). Statistical thermodynamic foundation for photovoltaic and photothermal conversion. IV. Solar cells with larger-than-unity quantum efficiency revisited, *Journal of Applied Physics*, Vol. 89, No.4, (February 2001), pp.2482-2490, ISSN 0021-8979.

Bazarov I.P. (1964).*Thermodynamics*, Pergamon Press, ISBN 978-0080100050, Oxford, Great Britain.

Berg J.M., Tymoczko J.L. & Stryer, L. (2010). *Biochemistry*, Freeman W. H. & Company, ISBN: 1429229365, ISBN-13: 9781429229364, New York, USA.

Chernin A.D. (2008). Dark energy and universal antigravitation. *Phys. Usp.* Vol. 51, No. 3, pp. 253–282, ISSN: 1063-7869(Print), 1468-4780(Online).

Couture L. & Zitoun R. (2000). *Statistical Thermodynamics and Properties of Matter*, Gordon and Breach, ISBN 9789056991951, Amsterdam, Holland.

Curzon F. & Ahlborn B. (1975). Efficency of a Carnot engine at maximum power output, *American Journal of Physics,* Vol. 43, Issue 1, January 1975, pp. 22-24, ISSN 0002-9505.

Datta S. (2006). *Quantum transport: Atom to Transistor*, Cambridge Univ. Press, ISBN 0-521-63145-9, Cambridge, Great Britain.

De Vos A.et al. (1993). Entropy fluxes, endoreversibility, and solar energy conversion, *Journal of Applied Physics,* Vol. 74, No. 6, (June 1993), pp.3631-3637, ISSN 0021-8979.

De Vos A. (1992). *Endoreversible thermodynamics of solar energy conversion*, Oxford Univ. Press, ISBN 978-0198513926, Oxford, Great Britain.

De Vos A. (1985). Efficiency of some heat engine at maximum-power conditions, *Am. J. Phys.*, Vol. 53, Issue 6, pp. 570-573, ISSN 0002.9505.

Dreicer H. (1964). Kinetic Theory of an Electron-Photon Gas, *Phys. Fluids*, Vol. 7, No. 5, pp. 732-754, Print: ISSN 1070-6631 Online: ISSN 1089-7666.

Dubinov A.E. (2009). Exact stationary solution of the Kompaneets kinetic equation. Точное стационарное решение кинетического уравнения Компанейца, Technical Physics Letters, Vol.35, No.3, pp.260-262. *Письма в ЖТФ*, том 35, вып.6, С.25-30, ISSN: 0320 - 0116.

Ferry D. & Goodnick S. (2005). *Transport in Nanostructures*, Cambridge Univ. Press, ISBN 0-521-66365-2, Cambridge, Great Britain

Green B. (2004). *The fabric of the cosmos: space, time, and the texture of realiti*. Alfred A. Knoff, ISBN 978-5-397-00001-7, New York, USA.

Han H., Bach U. & Cheng Y., Caruso R.A. 2007. Increased nanopore filling: Effect on monolithic all-solid-state dye-sensitized solar cell. *Applied Physics Letters*, Vol. 90, No.21, (May 2007), pp.213510-1-3, ISSN 0003-6951.

Hitz B. (2007). Mid-IR Fiber Laser Achieves ~10 W, *Photonics Spectra*, Vol. 41, No. 9, pp. 21–23. ISSN: n.d.

Ivanov K.P. (2008). Energy and Life. Энергия и жизнь, *Успехи современной биологии* (*Usp. Sovrem. Biol*), Vol. 128, No. 6, pp. 606–619. ISSN Print: 0042-1324

Johnson D.C., Ballard I.M. & Barnham K.W.J., Connolly J.P., Mazzer M., Bessière A., Calder C., Hill G., Roberts J.S. (2007). Observation of the photon recycling in strain-balanced quantum well solar cell. *Applied Physics Letters*, Vol. 90, No.21, (May 2007), pp.213505-1-3, ISSN 0003-6951.

Klaers J., Schmitt J., & Vewinger F., Weitz M. (2009). Bose–Einstein condensation of photons in an optical microcavity. *Nature*, Vol. 468, pp. 545-548, doi:10.1038/nature09567. ISSN: 0028-0836.

Kompaneets A.S., (1957). The establishment of thermal equilibrium between quanta and electrons, *Soviet Physics - JETP*, Vol. 4, No. 5, pp. 730-740, ISSN: 0038-5646.

Kondepudi D. & Prigogin I. (1998). *Modern Thermodynamics: From Heat Engines to Dissipative Structure*, John Wiley & Sons, Inc., ISBN 5-03-765432-1, New York, USA.

Kozar T. V., Karapuzova N. A. & Laptev G. V., Laptev V. I., Khlyap G. M., Demicheva O. V., Tomishko A. G., Alekseev A. M. (2010). Silicon Solar Cells: Electrical Properties of Copper Nanoclusters Positioned in Micropores of Silver Stripe-Geometry Elements, *Nanotechnologies in Russia*, Vol. 5, № 7-8, p.549-553, DOI: 10.1134/S1995078010070165, ISSN: 1995-0780 (print), ISSN: 1995-0799 (online).

Kuz'min V.A. & Shaposhnikov M.E. (1978). Condensation of photons in the hot universe and longitudinal relict radiation, *JETP Lett.*, Vol. 27, No. 11, pp.628-631, ISSN: 0370-274X.

Landsberg, P.T. & Leff, H. (1989). Thermodynamic cycles with nearly universal maximum-work efficiencies. *Journal of Physics A*, Vol. 22, No.18, (September 1989), pp.4019-4026. ISSN 1751-8113(print).

Landsberg P.T. & Tonge G. (1980). Thermodynamic energy conversion efficiency, *Journal of Applied Physics,* Vol. 51, No. 7, (July 1980), pp. R1-R20, ISSN 0021-8979.

Landsberg P.T. (1978). *Thermodynamics and statistical mechanics*. Oxford University Press, ISBN 0-486-66493-7, Oxford, Great Britain.

Landsberg P.T. (1977). A note on the thermodynamics of energy conversion in plants, *Photochemistry and photobiology*, Vol. 26, Issue 3, pp. 313-314, Online ISSN: 1751-1097.

Laptev V.I. (2010). Chemical Potential and Thermodynamic Functions of Thermal Radiation, *Russian Journal of Physical Chemistry A*, Vol. 84, No. 2, pp. 158–162, ISSN 0036-0244.

Laptev V.I. (2009). Thermodynamic Scale of the Efficiency of Chemical Action of Solar Radiation. *Doklady Physical Chemistry,* Vol. 429, Part 2, pp. 243–245, ISSN 0012-5016.

Laptev V.I. (2008). Solar and heat engines: thermodynamic distinguish as a key to the high efficiency solar cells, In: *Solar Cell Research Progress*, Carson J.A. (Ed.), pp. 131–179, Nova Sci. Publ., ISBN 978-1-60456-030-5, New York, USA.

Laptev V.I. & Khlyap H. (2008). High-Effective Solar Energy Conversion: Thermodynamics, Crystallography and Clusters, In: *Solar Cell Research Progress*, Carson J.A. (Ed.), pp. 181–204, Nova Sci. Publ., ISBN 978-1-60456-030-5, New York, USA.

Laptev V.I. (2006). The Special Features of Heat Conversion into Work in Solar Cell Energy Reemission. *Russian Journal of Physical Chemistry,* Vol. 80, No. 7, pp. 1011–1015, ISSN 0036-0244.

Laptev V.I. (2005). Conversion of solar heat into work: A supplement to the actual thermodynamic description, *J.Appl. Phys*., Vol. 98, 124905, DOI: 10.1063/1.2149189, ISSN 0021-8979(print), 1089-7550 (online).

Leff H. (1987). Thermal efficiency at maximum work output: New results for old heat engines. *American Journal of Physics,* Vol. 55, Issue 7, July 1987, pp.602-610, ISSN 0002-9505.

Lehninger A.L., Nelson D.L. & Cox M.M. (2008). *Lehninger Principles of Biochemistry*, 5th ed., Freeman, ISBN: 1572599316, ISBN-13: 9781572599314, New York, USA.

Lukash V.N, Rubakov V.A. (2008). Dark energy: myths and reality. Phys. Usp. Vol. 51, No. 3. pp. 283–289. ISSN: 1063-7869(Print), 1468-4780(Online).

Luque A. & Marti A. (2003). In: *Handbook of Photovoltaic Science and Engineering*, Luque A. & Hegedus S.(Eds.), John Wiley and Sons Ltd., ISBN: 978-0-471-49196-5. pp. 113-151, New York, USA.

Mazenko G.F. (2000). *Equilibrium Statistical Mechanics*, Wiley & Sons, Inc, ISBN 0471328391, New York, USA.

Muenster A. (1970). *Classical Thermodynamics*, Wiley-Interscience, ISBN: 0471624306, ISBN-13: 9780471624301, New York, USA.

Novikov I. (1958). The efficiency of atomic power stations. *Journal of Nuclear Energy,* Vol. 7, No. 1-2, (August 1958), pp.125-128.

Odum E.P. (1983). *Basic Ecology*, CBS College Publ., ISBN: 0030584140, ISBN-13: 9780030584145 New York, USA.

Pechurkin N.S. (1988). *Energiya i zhizn'* (Energy and Life), Nauka, Novosibirsk, Russia.

Peleshchak R.M. & Yatsyshyn V.P. (1996). About effect of inhomogeneous deformation on electron work function of metals, *Physics of Metals and Metallography*, MAIK Nauka Publishers – Springer, vol. 82, No. 3, pp.18-26, ISSN Print: 0031-918X, ISSN Online: 1555-6190.

Pillai S , Catchpole K.R. & Trupke T., Green M.A. (2007). Surface plasmon enhanced silicon solar cells, *Journal of Applied Physics,* Vol. 101, No.9, (May 2007), pp. 093105-1-8, doi:10.1063/1.2734885, ISSN: 0021-8979 (print), 1089-7550 (online)

Raven P.H.; Evert, R.F. & Eichhorn S.E. (1999). *Biology of Plants*. 6nd ed., Worth Publiscers, Inc., ISBN: 1572590416, USA.

Rhoderick E. H., (1978). *Metal-semiconductor contacts*. Clarendon Press, ISBN 0198593236, Oxford, Great Britain.

Rubin M. (1979). Optimal configuration of a class of irreversible heat engines. I. *Physical Review A*, Vol. 19, No. 3, (March 1979), pp.1272-1276. ISSN 1094-1622 (online), 1050-2947 (print).

Semenchenko V.K. (1966). *Избранные главы теоретической физики*, Просвещение, Москва.

Shockley W.; Queisser H., (1961). Detailed Balance Limit of Efficiency of *p-n* Junction Solar Cells, *J. Appl. Phys.*, , 32, 510-519. ISSN 0021-8979.

Slaoui A. & Collins R.T. (2007). Advanced Inorganic Materials for Photovoltaics. *MRS Bulletin*, Vol. 32, No.3, pp.211-214, ISSN: 0883-7694.

Spavieri G. & Rodrigues M. (2007). Photon mass and quantum effects of the Aharonov-Bohm type, *Phys. Rev. A*, Vol. 75, 05211, ISSN 1050-2947 (print) 1094-1622 (online).

Steinfeld A. & Palumbo R. (2001). *Encyclopedia of Physical Science & Technology*. R.A. Mayers (Editor)Vol. 15, pp. 237–256, Academic Press, ISBN: 0122269152, ISBN-13: 9780122269158, New York.

Sze S.M. & Ng, K.K. (2007). *Physics of semiconductor devices*, J. Wiley & Sons, Inc., ISBN 0-471-14323-5, Hoboken, New Jersey, USA.

Voet D.J., Voet J.G. & Pratt C.W. (2008). *Principles of Biochemistry*, 3d ed., John Wiley & Sons Ltd, ISBN:0470233966, ISBN-13: 9780470233962, New York,USA.

Wegh R.T., Donker, H. & Oskam K.D., Meijerink A. (1999). Visible Quantum Cutting in $LiGdF_4:Eu^{3+}$ Through Downconversion, *Science*, 283, 663-666, *DOI:10.1126/science.283.5402.663*, ISSN 0036-8075 (print), 1095-9203 (online).

Werner J.; Kolodinski S. & Queisser H. (1994). Novel optimization principles and efficiency limits for semiconductor solar cells. *Physical Review Letters,* vol.72, No.24 (June 1994), p.3851-3854. ISSN 0031-9007 (print), 1079-7114 (online)

Weymann R. (1965). Diffusion Approximation for a Photon Gas Interacting with a Plasma via the Compton Effect , *Phys. Fluids*, Vol. 8, No. 11, pp. 2112-2114, Print: ISSN 1070-6631 Online: ISSN 1089-7666.

Wuerfel P. (2005). *Physics of Solar Cells*, WILEY-VCH Verlag GmbH and Co. KGaA, ISBN 978-3527408573, Wienheim, Germany.

Yungman V.S. & Glushko (Eds). (1999). *Thermal Constant of Substances*, 8 volume set, Vol. 1, John Wiley & Sons, ISBN: 0471318558 New York, USA.

Zel'dovich Ya.B. & Syunyaev R.A. (1972). Shock wave structure in the radiation spectrum during bose condensation of photons, *Soviet Physics - JETP*, Vol. 35, No. 1, pp. 81-85, ISSN: 0038-5646.

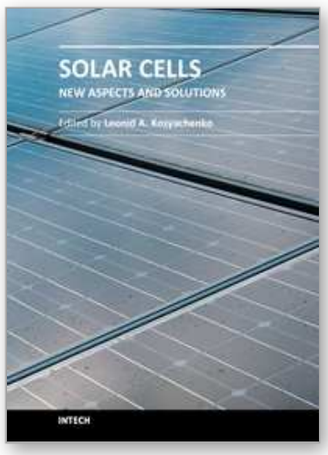

Solar Cells - New Aspects and Solutions

Edited by Prof. Leonid A. Kosyachenko

ISBN 978-953-307-761-1
Hard cover, 512 pages
Publisher InTech
Published online 02, November, 2011
Published in print edition November, 2011

The fourth book of the four-volume edition of 'Solar cells' consists chapters that are general in nature and not related specifically to the so-called photovoltaic generations, novel scientific ideas and technical solutions, which has not properly approved. General issues of the efficiency of solar cell and through hydrogen production in photoelectrochemical solar cell are discussed. Considerable attention is paid to the quantum-size effects in solar cells both in general and on specific examples of super-lattices, quantum dots, etc. New materials, such as cuprous oxide as an active material for solar cells, AlSb for use as an absorber layer in p-i-n junction solar cells, InGaAsN as a promising material for multi-junction tandem solar cells, InP in solar cells with MIS structures are discussed. Several chapters are devoted to the analysis of both status and perspective of organic photovoltaics such as polymer/fullerene solar cells, poly(p-phenylene-vinylene) derivatives, photovoltaic textiles, photovoltaic fibers, etc.

InTech Europe
University Campus STeP Ri
Slavka Krautzeka 83/A
51000 Rijeka, Croatia
Phone: +385 (51) 770 447
Fax: +385 (51) 686 166
www.intechopen.com

InTech China
Unit 405, Office Block, Hotel Equatorial Shanghai
No.65, Yan An Road (West), Shanghai, 200040, China
中国上海市延安西路65号上海国际贵都大饭店办公楼405单元
Phone: +86-21-62489820
Fax: +86-21-62489821

IntechOpen